The Pennsylvania State University
The Graduate School

PREPARATION AND CHARACTERIZATION OF N-ALKYL QUATERNIZED ACTIVATED CARBON FOR PERCHLORATE REMOVAL FROM GROUNDWATER

A Thesis in
Forest Resources
by
Xin Gu

Submitted in Partial Fulfillment
of the Requirements
for the Degree of

Master of Science

December 2011

The thesis of Xin Gu was reviewed and approved* by the following:

Nicole R. Brown
Associate Professor of Wood Chemistry
Thesis Advisor

Fred S. Cannon
Professor of Environmental Engineering

Seong H. Kim
Associate Professor of Chemical Engineering

Michael G. Messina
Professor of Forest Resources
Director, School of Forest Resources

*Signatures are on file in the Graduate School.

Abstract

Chemicals that are released into our surface and subsurface waters are a pervasive environmental problem. Sources of chemical contamination range from incorrectly disposing of and treating chemical waste, to abandoned waste disposal sites, to leaking storage tanks that might contain hazardous chemicals. Perchlorate is one of those contaminants that, due to kinetic and thermodynamic properties, is quite difficult to remove from contaminated waters and soils. Because of this, perchlorate has become a significant environmental contaminants. Conventional treatment techniques, including virgin granular activated carbon (GAC), air stripping and advanced oxidation had limited or no effect on low perchlorate concentrations in water. Ion exchange with quaternary ammonium or pyridinium groups is currently the most frequently used method for the treatment of perchlorate-contaminated drinking water. This study aims to prepare activated carbon tailored with pyridinium functional groups to remove perchlorate from ground water.

To achieve this aim, three main phases of research activities were conducted. In Phase I, activated carbon with pyridinium functional groups and high pore volume was prepared. The sample preparation included three steps: nitric acid oxidation, thermal treatment in ammonia and the quaternization reaction. The surface chemistry and pore structure of samples from each step were characterized (phase II) and the reaction conditions were optimized. In phase III, the final products were tested with respect to perchlorate adsorption (isotherm test and rapid small scale column test).

The nitric acid oxidation generated a large number of surface functional groups such

as carbonyl, carboxyl, and phenol groups, which is a prerequisite for introducing a high amount of nitrogen containing moieties onto the carbon surface. During the second step of the treatment, amination, surface elemental analysis (by X-ray photoelectron spectroscopy, XPS) results showed that nitrogen was incorporated into the carbon matrix as high as 7.2% (atomic percentage). The temperature of the ammonia treatment, the degree of pre-oxidation and the fraction of ammonia in the carrier gas influenced the resulting populations of oxygen and nitrogen species. Based on the XPS study on N1s spectrum at different amination temperature, it is suspected that during the initial stages of heating, some intermediates such as amide, lactam and imide were formed. As temperature increased, these labile species were converted to more thermodynamically stable structures with heterocyclic aromatic moieties (pyridinic or pyrrolic functional groups). At higher temperature ($>$ 600 °C), the fraction of quaternary nitrogen gradually increased and some nitrogen species might have decomposed. Through quaternization, pyridine groups at edge sites were successfully transformed to pyridinium groups (20% of total nitrogen). XPS in conjunction with chemical derivatization (by methyl iodide) was confirmed to be an effective way to qualitatively analyze the pyridinium species. Pyridinium-tailored carbon achieved as much as a 6-fold improvement in bed life for adsorbing perchlorate as determined by rapid small-scale column tests (RSSCT) using spiked groundwater with perchlorate (30 ppb).

Table of Contents

List of Figures

List of Tables

Nomenclature

ACF	Activated Carbon Fibers
ASAP	Accelerated Surface Area and Porosimetry
ASTM	The American Society for Testing Materials
BE	Binding Energy
BET	Brunauer-Emmett-Teller
CCL	Contaminants Candidate List
CNT	Carbon Nanotube
DFT	Density Functional Theory
DRIFTS	Diffusion Reflectance FTIR Spectroscopy
EBCT	Empty Bed Contact Time)
FTIR	Fourier Transform Infrared Spectroscopy
GAC	Granular Activated Carbon
GO	Graphene Oxide
IX	Ion Exchange
IUPAC	International Union of Pure and Applied Chemistry
MCL	Maximum Contaminant Limit
MDL	Method Detection Limit
MWCNTs	Multi-Walled Carbon Nanotubes

pH_{zpc}	pH-Zero Point of Charge
PWS	Public Water Systems
RSSCTs	Rapid Small-Scale Column Tests
TPD	Temperature Programmed Desorption
VOCs	Volatile Organic Compounds
XPS	X-ray Photoelectron Spectroscopy

Chapter 1

Introduction and Justification

1.1 Executive summary

Several significant regions of America's groundwater sources are contaminated with perchlorate, nitrate, sulfate, chromate, vanadate, and radioactive oxyanions. For example, perchlorate taints the groundwater that 15 million Americans might otherwise drink (Logan, 2001). Perchlorate has been shown to inhibit the uptake of iodide by the thyroid, leading at least eight states to develop nonregulatory action levels or advisories for perchlorate ranging from 1 part per billion to 51 parts per billion (ppb) (U.S. General Accountability Office, 2007). Although perchlorate is thermodynamically reactive, it is kinetically stable in groundwater at low concentrations. Therefore, once it enters the groundwater, it remains there for long durations.

Activated carbon is a commonly used technology throughout the water treatment industry. However, virgin activated carbon was shown to be ineffective at removing perchlorate from groundwater partially due to the oxygen functional groups bearing negatively charged sites on the carbon surface. The objective of our project is to functionalize activated carbon with the quaternary positively charged ammonium functional group to remove perchlorate from groundwater.

1.2 Background on perchlorate

The perchlorate ion can be associated as a salt with such cations such as ammonium, potassium and sodium. The majority of perchlorate salts are in the form of ammonium perchlorate, which is a strong oxidant that is used in rocket and missile engines as

solid propellants. Perchlorate salts are also used in pyrotechnics, matches, munition, chemical analytical industries, lubricating oils, aluminum refineries, dyes and airbag inflators. Perchlorate salts are also found in fertilizer either through natural or manmade contamination. In 1998, ammonium perchlorate production was 4,000 tons per year (Urbansky, 2002). To date there are 162 facilities in 36 states that either produce or use perchlorate compounds (Brandhuber & Clark, 2005). Perchlorate also originates naturally from sources such as soils in hot dry climates, potassium ore deposits, and degradation of other compounds such as sodium hypochlorite.

Perchlorate salts are very soluble and will dissociate to form their corresponding cations and the perchlorate anion. The perchlorate anion is very mobile in aqueous systems and is very stable. This is because of the slow reduction of the central chlorine atom. The tetrahedral symmetry of perchlorate coupled with its even charge distribution, allows the anion to have low affinity to soils and minerals. It is these characteristics that make perchlorate ubiquitous in surface and ground waters in many states.

Prior to 1997, perchlorate was discharged into sewage systems or natural waters without any treatment. Shortly after the development of the low level analytical method, perchlorate began to be detected in ground and surface drinking water supplies across the country (Srinivasan & Sorial, 2009). Perchlorate occurrence in drinking water is national in scope: it has been detected in drinking water in 26 states and Puerto Rico (Kucharzyk et al., 2009). Geographically, the highest density of perchlorate detection is in Southern California, west central Texas, along the east coast between NewJersey and Long Island, and in Massachusetts. California public water suppliers detected 33 out of the 110 investigated wells had perchlorate concentration greater than 18 μg/L, with the highest concentration at 280 μg/L (Motzer, 2001).

The major concern of perchlorate is the competition with iodine uptake by the thyroid gland for both humans and animals. The perchlorate anion blocks the protein that acts as an iodide pump to the thyroid gland. Studies have shown that exposure to perchlorate in pregnant women can result in serious and irreversible effects on the fetus (Srinivasan & Viraraghavan, 2009). Extensive animal toxicity testing has been performed to study the health effects of perchlorate in human beings. U.S. EPA has included perchlorate in the Contaminants Candidate List (CCL) with a reference dose of 0.7 μg/kg/day, which corresponds to a drinking water equivalent level of 24.5 ppb (Kucharzyk et al., 2009).

1.3 Perchlorate removal

A significant amount of research has been performed to evaluate treatment alternatives for perchlorate remediation in drinking water in the last decade. Substantial advances in perchlorate treatment such as biological and chemical reduction have been made (Logan, 2001). However, these methods still have limited applications in drinking water purification due to either low reaction rates or the use of huge amounts of metals, as in the case of chemical reduction. Among alternatives for perchlorate removal, ion exchange is apparently the most efficient method. However, additional operational issues and large quantities of waste (brine solution and disposed resin) make the ion exchange resins inefficient for the low concentration of perchlorate in groundwater.

Activated carbon adsorption is a cost effective technique for removing organic contaminants and, less frequently, for adsorbing inorganics from water. Although virgin activated carbon could remove perchlorate, its removal capacity was found to be low (Na et al., 2002; Mahmudov & Huang, 2010). Nonetheless, activated carbon does offer the advantage of having large surface area, and after appropriate surface modifications it has been shown to be competitive for perchlorate removal.

Herein, research has focused on modifying the carbon surface with N-alkyl quaternized functionality so that the carbon achieves higher adsorption capacity for perchlorate from natural water, without undermining the pore structure that is beneficial to perchlorate adsorption. This research addresses the application potential of the quaternary N-tailored carbon and the adsorption mechanism of the anion, which will be important for society. Also, this research may help to solve one of world's emerging challenges-providing clean sustainable water for a growing population.

Chapter 2

Literature Review

2.1 Perchlorate as a new contaminant

2.1.1 Property, usage and occurrence of perchlorate

The perchlorate anion consists of a tetrahedral array of oxygen atoms around a central chlorine atom. Perchlorate is the anionic component of a salt most often associated with the cations ammonium, sodium, or potassium. Because of its symmetry, and the fact that the charge -1 is distributed evenly across the outer oxygen atoms, the perchlorate ion has a low charge density and interacts weakly with most cations (Hagström, 2006). Perchlorate salts have low vapor pressure and hence cannot volatilize under ambient conditions. Perchlorate salts are highly soluble in water and dissolved perchlorate anions do not tend to partition from aqueous to gas phase ($\log K_{OW} \ll 0.0$) (Gu & Coates, 2006). Thermodynamic measurements indicate perchlorate anion as a strong oxidant, however slow kinetics generally limit its reactivity in typical ambient environments, and thus, chemical reduction is not observed in subsurface environments, even under highly reducing conditions. This strong oxidant potential and low reactivity nature allows perchlorate salts to persist in the environment. They are hard to treat by chemical reduction, while biologically mediated reactions can effectively degrade them (Srinivasan & Viraraghavan, 2009).

Perchlorate contamination in both ground and surface water mainly originates from facilities that manufacture or use ammonium, potassium or sodium perchlorate salts for various purposes (Urbansky, 2002). The majority of perchlorate salts are in the form of ammonium perchlorate, which is a strong oxidant used in rocket and missile engines as a solid propellant. Perchlorate salts are also used in pyrotechnics, matches,

munitions, chemical analytical industries, lubricating oils, aluminum refineries, dyes and airbag inflators. Perchlorate salts are also found in fertilizer either through natural or manmade contamination. In 1953, ammonium perchlorate production was 2,000 tons per year. By the mid 1980s production peaked at 15,000 tons per year, and then declined to 4,000 tons per year in 1998 (Urbansky, 2002). This decline was mainly due to the short shelf life, requiring periodic replacement of rockets and missiles, thus reducing the quantities that are used in rocket boosters or missiles. As of 2005, there were 162 facilities in 36 states that either produce or use perchlorate compounds (Brandhuber & Clark, 2005).

As discussed above, perchlorate is highly soluble in water and stable under normal atmospheric conditions. Once a perchlorate compound is released into the environment, most often into bodies of water, it dissolves. Due to its limited ability to adsorb onto surfaces, perchlorate is transported through bulk movement of water and mixing processes (Gu & Coates, 2006). Because perchlorate is inert in groundwater and surface water, contamination can persist for long periods of time. The tetrahedral symmetry of perchlorate, coupled with the even charge distribution, allows the anion to have low affinity to soils and minerals. It does not readily sorb to clays even though clay has some amount of cation exchange capacity. The fate of perchlorate, if not remediated or treated, is dependent on hydrologic as well as biological factors. The biological transformation of perchlorate has been widely studied. Microorganisms, specifically bacteria, that can transform perchlorate are abundant in nature. Microbial degradation of perchlorate in soil and water occurs mostly under anaerobic conditions, and can be affected by competing electron acceptors such as nitrate and chlorate, as well as organic matter (Logan, 2001).

Recall that prior to 1997, the perchlorate anion could not be detected at concentrations below 100 μg/L. However, soon after the California Department of Health developed an analytical method that could detect perchlorate at concentrations as low as 4 μg/L, perchlorate was observed in water sources that were previously considered uncontaminated.

In the U.S., perchlorate contamination has been found in the United States has been associated with military activities or defense contractors. In the state of Nevada, perchlorate contamination was observed at concentrations up to 3.7 g/L in the groundwater, which was traced back to two ammonium perchlorate manufacturing facilities (Urbansky, 1998). This resulted in perchlorate contamination of Lake Mead surface water, a significant water source for the Southwestern United states. The contamination affected 15-20 million people in Arizona, southern Nevada, and southern California. A recent study to determine the overall distribution of perchlorate in California drinking water

sources found that the mean perchlorate level was 3.6 μg/L, and among sources with positive perchlorate results, the mean level was 12 μg/L (Brandhuber & Clark, 2005).

2.1.2 Toxicity and regulation of perchlorate

As noted previously, perchlorate interferes with iodide uptake into the thyroid gland. Because iodide is an essential component of thyroid hormones, perchlorate disrupts how the thyroid functions. In adults, the thyroid helps to regulate the metabolism. In children, the thyroid plays a major role in proper development, in addition to metabolism. Impairment of thyroid function in pregnant mothers may impact the fetus and result in such effects as changes in behavior, delayed development and decreased learning capability. Perchlorate in drinking water or ingested by other means leads to inhibition of iodine uptake (as iodide) into thyroid. This is a competitive inhibition and therefore reversible when exposure to perchlorate ceases (Charnley, 2008).

To determine the health effects of perchlorate in humans, fairly extensive animal toxicity studies have been conducted (Kucharzyk et al., 2009). Paulus et al. (2007) studied the inhibition of iodide uptake in rats exposed to perchlorate, finding that perchlorate significantly impacted iodide uptake in normal rats. Liu et al. (2008) found that perchlorate exposure in addition to influencing thyroid function, increased arsenate toxicity and also resulted in significant growth retardation in zebra fish.

In 1998, the U.S. EPA added perchlorate to the drinking water contaminant candidate list (CCL) based on its presence in drinking water supplies in the southwestern United States. In 2005, the United States National Academy of Sciences produced a report on the health implications of perchlorate ingestion, which has been used by the U.S. EPA to establish an oral reference dose of 0.0007 milligrams perchlorate per kilogram body weight per day and a drinking water equivalent level (DWEL) of 24.5 μg/L (Zewdie et al., 2010). U.S. EPA is expected to issue a final regulatory determination for perchlorate based on further advice from the National Academy of Sciences. Various states in the United States have implemented guidelines or goals ranging from 1 μg/L to 18 μg/L for perchlorate in drinking water (Srinivasan & Viraraghavan, 2009).

In 2009, a study was conducted to estimate the national cost implications of setting a federal maximum contaminant limit (MCL) for perchlorate at levels between 4 and 24 μg/L (Russell et al., 2009). The results showed that only 3.4% of public water systems (PWS) would be affected by a perchlorate MCL of 4 μg/L and less than 1% of PWSs would be required to treat their water at an MCL of 24 μg/L. At an MCL of 4 μg/L, total net present value compliance costs are estimated to be 2.1 billion U.S. dollars. At

MCL of 24 μg/L, the estimated compliance cost drops to 0.1 billion U.S. dollars.

2.1.3 Perchlorate treatment technologies

Treatment technologies that are used to remediate perchlorate are usually in the form of the separation and destruction process (Gu & Coates, 2006). Typically, the separation treatment method is for the remediation of ground and surface water that is contaminated with perchlorate, while the destruction method is for soils. Because of its physical characteristics (i.e. low reactivity, low volatility, high solubility), typical water treatment technologies, including air stripping and advanced oxidation, are not effective options for perchlorate removal. The most common and more successful physical treatment is an ion exchange process. The success of the physical adsorption method over chemical and biological reduction processes is due to perchlorate's kinetic and thermodynamic properties.

2.1.3.1 Perchlorate removal by ion exchange resin

Ion exchange is the most-proven and widely-accepted physical process technology to meet existing perchlorate treatment goals. Ion exchange is a process by which ions of a given species are displaced from an insoluble exchange material by ions of a different species in solution. The net result is that the targeted ions are removed from water through sorption onto resins. Ion exchange has been successfully used since the 1940s for drinking water treatment (softening and deionization) and other industrial processes. Many different types of cation and anion exchange products prepared as resins are commercially available. This technology was one of the first ex-situ technologies considered for remediation of perchlorate-contaminated waters. While other ex-situ and in-situ technologies have been developed and are undergoing evaluation, ion exchange remains a proven and accepted technology.

Although conventional ion exchange resins are capable of removing perchlorate, the effectiveness is hampered due to competing anions. Also, organics, TDS, calcium, or iron in the influent can clog resin beds and reduce system effectiveness. Therefore, selective resins are preferred for treatment of perchlorate in water. In addition, the use of selective ion-exchange technology offers other advantages such as the following: (1) the treatment process does not change the water chemistry by adding or removing chemicals or nutrients because the perchlorate anions are selectively or preferentially removed over other competing anions, and (2) the treatment system can be operated at a relatively high flow rate, typically at about 0.5 to 2 empty bed volumes per minute, and therefore

requires only a relatively small treatment unit.

Both the functionality and the type of matrix affect the perchlorate removal efficiency. Tripp & Clifford (2006) observed that polyvinylpyridine resins were highly selective for perchlorate, followed by polystyrene resins, and the least selective were polyacrylic resins. Most Type I strong-base anion-exchange resins exhibit a relatively high selectivity for perchlorate because perchlorate is larger and has lower hydration energy than most other anions encountered in groundwater (such as NO_3^-, Cl^-, SO_4^{2-}, and HCO_3^-). Unlike the Type II resins, the increasing order of affinity of singly-charged ions for Type I strong-base anion-exchange resins is bicarbonate < chloride < nitrate < perchlorate. Therefore, there is a natural bias toward exchanging perchlorate preferentially over the other anions in the solution, and this natural bias can be further enhanced by chemical modification of the resin. Such modifications include altering the size and shape of the cationic exchange sites and altering the polymer cross-link density on the resin. Under the U.S. Department of Energy's (DOE's) sponsorship, the Oak Ridge National Laboratory (ORNL) recently developed a new class of highly selective anion exchange resins that were shown to effectively remove large, poorly hydrated anions (such as perchlorate and pertechnetate (TcO_4^-)) to a nondetectable level. This new class of anion-exchange resins is called "bifunctional" anion-exchange resins because they have two quaternary ammonium groups, one having long chains for enhanced selectivity and one having shorter chains for improved sorption kinetics (Figure 2.1). At an influent concentration of about 450 μg/L perchlorate, the bifunctional anion-exchange resin bed treated approximately 40,000 empty bed volumes of groundwater before a significant breakthrough of perchlorate occurred (Gu et al., 2002). Similarly, Xiong et al. (2007) studied perchlorate sorption capacity for different types of ion exchange resins: standard strong-base anion (SBA), weak-base anion (WBA) exchangers, a bifunctional resin (A-530E), a class of polymeric ligand exchangers (PLEs), and an ion-exchange fiber (IXF). While A-530E offered the greatest perchlorate capacity and selectivity, practically acceptable capacity was also observed for styrenic SBA and WBA resins, a PLE, and IXF. In contrast, polyacrylic resins offered much lower perchlorate capacity. The greater capacity of styrenic resins is attributed to enhanced ion-pairing and Lewis acid-base interaction due to the hydrophobic nature of polystyrene matrices and the lower hydration energy of perchlorate.

Although the selective ion-exchange technology and resins have been available for years, the application of these selective resins for groundwater treatment with perchlorate contamination has been limited until recently. This was primarily because of the difficulty in regenerating these resins. As discussed in the previous section, because perchlorate anions are selectively and strongly sorbed, regeneration of spent resin becomes

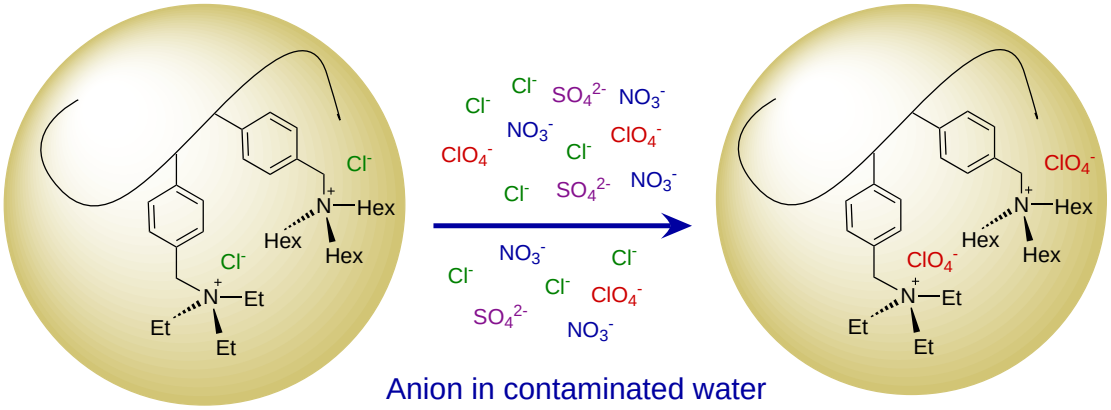

Figure 2.1: Bifunctional resin for selective sorption of perchlorate (Gu et al., 2002)

particularly challenging and costly using conventional NaCl brine regeneration technology. The exceptionally high affinity of perchlorate for these resins makes it practically impossible to regenerate the spent resin even with large volumes of concentrated brine solutions (e.g., by using 12 percent NaCl brine) (Gu & Coates, 2006). The use of large volumes of brine translates into both a high operating cost and waste-disposal problems associated with the brine containing perchlorate. The research group in the Oak Ridge National Laboratory developed a regeneration method for the above-mentioned bifunctional resins (Gu et al., 2001). By applying a solution containing 1 M $FeCl_3$ and 4 M HCl, nearly 100% of loaded perchlorate was desorbed after 5 bed volumes of regenerant. Its assumed that tetrachloraferrate ($FeCl_4^-$) was the dominant species in the regeneration solution, since perchlorate has a similar structure to tetrachloraferrate. It was surmised that perchlorate was easily displaced from the ion exchange resin by tetrachloraferrate. The small amount of regenerant necessary (5 bed volumes) to achieve the regeneration means that less brine waste was produced. No significant loss of perchlorate capacity was observed following several regeneration cycles.

Perchlorate is separated, but not destroyed, during the ion exchange process, thus subsequent disposal of both the perchlorate and any waste products are needed. The destruction of perchlorate and nitrate in regenerant brines can be accomplished by either microbial or chemical procedures. Gu et al. (2007) developed a method to completely destroy perchlorate in $FeCl_3$-HCl solution by solid-phase ferrous Fe(II) (as $FeCl_2 \cdot 2\,H_2O$). Perchlorate was found to decompose into non-hazardous Cl^- and water under certain catalytic conditions and a complete reaction occurs within a few hours to one day with an initial perchlorate concentration 87 to 91 mmol/L. The rate constant for the pseudo-first-order reaction increased nearly three orders of magnitude when the temperature was increase from 110 to 195 °C, and a complete reduction of perchlorate occurred in less

than 1 hour at 195 °C. This method was applied to regenerating waste from ion exchange resins. The destruction process does not alter properties of the regeneration solution; so the resins could be reused. Xiao et al. (2010) used a salt tolerant, perchlorate-reducing culture to regenerate ion exchange resins exhausted with perchlorate. Degradation of perchlorate on, or around, the resin and in the bulk aqueous phase was completed in 5 h.

2.1.3.2 Perchlorate removal by activated carbon

Granular Activated Carbon (GAC) has a long and successful history of use in drinking water treatment. In the United States, GAC is generally used to combat taste and odor problems or to remove volatile organic compounds (VOCs) from groundwater and as a filtration media (American Water Works Association, 1999). One of the biggest advantages with GAC adsorption is that it is widely used in the drinking water treatment industry and would be easy to retrofit to target perchlorate in the water. Also, effective regeneration of the spent carbon makes this technology economically feasible (Srinivasan & Sorial, 2009).

Column tests by Na et al. (2002) revealed that there was no detectable perchlorate for about 1200 bed volumes using a bituminous GAC from Superior Adsorbents Inc. (Emlenton, PA). This was increased to 1500 bed volumes after modification by iron-preloading. Water used in this test was groundwater from the City of Redlands, CA, with a perchlorate concentration of approximately 75 ppb. 1200-1500 bed volumes represented about four to six weeks of operation when the EBCT (empty bed contact time) was 20 min at full scale. In contrast, the same GAC bed at the treatment plant was able to last 18 months for trichloroethylene removal before thermal reactivation.

Thermochemical treatment by ammonia is another way to form positively-charged surface sites such as RNH_3^+. The type of nitrogen functionalities created on the carbon surface largely depends on the conditions used during the amination or ammoxidation treatment. Some of the nitrogen functionalities are not thermally stable and differences among the samples can be explored according to treatment temperature. Chen et al. (2005a,b) found that ammonia thermal tailoring acted as an activating agent at temperatures higher than 500 °C, and it caused both physical and chemical changes to the carbons. Micropores were created in the process, which were reflected in the increase of surface area and micropore volume. The nitrogen content was increased through ammonia tailoring, thereby significantly increased the positive charge of the carbon surface, which is the most important surface property influencing adsorption. After the tailoring procedure, a 4-fold increase in bed volume to initial perchlorate breakthrough was observed. In another study the authors also looked at regeneration of the ammonia-tailored

GAC with ammonia and carbon dioxide (Chen & Cannon, 2005). When compared to steam regeneration, which resulted in loss of nitrogen and positive surface charge, regeneration with ammonia and carbon dioxide was able to preserve most of the nitrogen content and, hence, resulted in increased regeneration capacity for perchlorate adsorption.

Parette & Cannon (2005); Parette et al. (2005) found that the cationic surfactant with a quaternary ammonium functional group would increase the positive charge sites on the activated carbon. Surfactants consisted of an uncharged tail (alkyl chain) and a charged head (in this case a quaternary ammonium or pyridinium). The hydrophilic heads faced away from the carbon surface and away from the other alkyl tails. The surfactants were pre-loaded onto GAC by pumping a concentrated surfactant-water solution cyclically through a GAC bed. Tailoring the carbon increased the breakthrough time by a factor of 30 and up to 34,000 bed volumes could be treated before breakthrough. The authors were able to achieve these results with actual reservoir water in which other anions were present at a much higher concentration than perchlorate. The authors also tested other carbon sources such as the surfactant carrier and found the pore structure demonstrated the surfactant loading: with microporous structure the surfactant loading rate was low and with macroporous structure the surfactant was easier to leach. The authors recommended using a polishing virgin GAC bed following the surfactant tailored bed.

Mahmudov & Huang (2010) tested 10 types of commercial activated carbons, made from wood, bituminous coal, and lignite coal, for perchlorate adsorption characteristics using pH as the master variable. Results showed that surface charge, not specific surface area, was the most important factor governing perchlorate removal. All wood-based activated carbons that had large variation in specific surface area, e.g. 3-fold, but very close pH_{zpc} (surface charge) exhibited similar perchlorate adsorption capacity. On the other hand, the activated carbons having $pH_{zpc} > 8$ exhibited higher adsorption capacity than those with low pH_{zpc} of 2-3. This provided strong evidence of electrostatic forces as responsible for perchlorate adsorption. However, Yoon et al. (2009) claimed that perchlorate was associated with functional groups on GAC surfaces through interactions stronger than electrostatic interactions. So, the adsorption mechanism of perchlorate on GAC surface is still unclear.

2.2 Activated carbon

2.2.1 General introduction

The term activated carbon defines a group of materials with highly developed internal surface area and porosity and, hence, a large capacity for adsorbing chemicals from gases or liquids (American Water Works Association, 1999). Activated carbon has been used for purification purposes and in chemical production for centuries. The carbon is produced from a tremendous variety of carbonaceous-starting materials including bituminous coal, lignite coal, coconut shells, peach pits, sawdust, wood char, lignin, petroleum coke, peat, carbon black, etc. The following criteria are considered when choosing a carbonaceous raw material: (1) potential for obtaining high-quality activated carbon; (2) presence of minimum inorganics; (3) volume or cost of the raw material; (4) storage life of the raw material, and (5) workability of the raw material (Bansal & Goyal, 2005).

The first step in activated carbon production is carbonization. Carbonization is conducted at 600-650 °C in an inert atmosphere. Between 400 and 600 °C most organic solids undergo reactions leading to the loss of hydrogen and formation of free radicals, which condense to form a rigid, cross-linked solid char. The carbonization process causes some increase in porosity and modifies the pore structure inherent to the precursor (Bansal & Goyal, 2005).

The subsequent activation step helps to develop pore structure by selective gasification of carbon at 850-950 °C in steam or, CO_2, or a mixture of these. The removal of carbon atoms increases the average size of already existing pores and opens up closed porosity. Following activation, there is final screening and a de-dusting operation. Chemical activation is another way to increase porosity. Compounds such as $ZnCl_2$ and H_3PO_4 are added to the parent feed stock prior to carbonization. The reaction usually is carried out at temperatures in the range of 500-900 °C (Bansal & Goyal, 2005). The precursors are usually cellulosic materials such as wood. It is believed that chemicals attack the cellulosic structures in the precursor. Water is eliminated and cross-linking and increased aromatization are promoted during the carbonization. Chemically-activated carbons from wood have high pore volume, high surface area, and low bulk density (0.27 g/cm^3).

2.2.2 Activated carbon adsorption

Adsorption arises as a result of the unsaturated and unbalanced molecular forces that are present on every solid surface. Thus, when a solid surface is brought into contact

with a liquid or gas, there is an interaction between the fields of forces of the surface and that of the liquid or the gas. The solid surface tends to satisfy these residual forces by attracting and retaining on its surface the molecules, atoms, or ions of the gas or liquid. This results in a greater concentration of the gas or liquid in the near vicinity of the solid surface than in the bulk gas or vapor phase, despite the nature of the gas or vapor. The process by which this surface excess is caused is called adsorption. The adsorption involves two types of forces: physical forces that may be dipole moments, polarization forces, dispersive forces, or short range repulsive interactions and chemical forces that are valence forces arising out of the redistribution of electrons between the solid surface and the adsorbed atoms (Bansal & Goyal, 2005).

In the case of physical adsorption, the adsorbate is bound to the surface by relatively weak van der Walls forces, which are similar to the molecular forces of cohesion and are involved in the condensation of vapors into liquids. Chemisorption, on the other hand, involves exchange or sharing of electrons between the adsorbate molecules and the surface of the adsorbent resulting in a chemical reaction. The bond formed between the adsorbate and the adsorbent is essentially a chemical bond and is thus much stronger than in the physical adsorption. Physical adsorption is nonspecific and occurs between any adsorbate-adsorbent systems, but chemisorption is specific. The adsorption data can be represented by several isotherm equations, the most important being the Langmuir, the Freundlich, the Brunauer-Emmett-Teller (BET), and Dubinin equations. The first two isotherm equations apply equally to physisorption as well as to chemisorption. The BET and Dubinin equations are most important for the analysis of physical adsorption of gases and vapors on porous carbons.

The adsorption capacity of activated carbon for specific chemicals depends on the chemical and porous structures of the carbon, as well as on the chemical and physical characteristics of the adsorbate.

2.2.2.1 Pore structure

The activated carbons in general have a strongly-developed internal surface and are usually characterized by a polydisperse porous structure consisting of pores of different sizes and shapes. The porous structure formed during the carbonization process is developed further during the activation process, when the spaces between the elementary crystallites are cleared of tar and other carbonaceous material. The activation process enhances the volume and enlarges the diameters of the pores. The structure of the pores and their pore size distribution are largely determined by the nature of the raw material and the history of its carbonization.

It is now well accepted that activated carbons contain pores from less than a nanometer to several thousand nanometers in diameters. The classification of pores suggested by Dubinin and accepted by the International Union of Pure and Applied Chemistry (IUPAC) is based on their width, which represents the distance between the walls of a slit-shaped pore or the radius of a cylindrical pore. The pores in activated carbons are divided into three groups: the micropores with diameters less than 2 nm, mesopores with diameters between 2 and 50 nm, and macropores with diameters greater than 50 nm. The micropores constitute a large surface area (about 95% of the total surface area of the activated carbon) and micropore volume and, therefore, determine to a considerable extent the adsorption capacity of a given activated carbon, provided however that the molecular dimensions of the adsorbate are not too large to enter the micropores. The micropores are filled at low relative vapor pressure before the commencement of capillary condensation. The mesopores contribute to about 5% of the total surface area of the carbon and are filled at higher relative pressure with the occurrence of capillary condensation. Attempts, however, are now on to prepare mesoporous carbons. The macropores are not of considerable importance to the process of adsorption in activated carbons, as their contribution to surface area does not exceed 0.5 m^2/g. They act as conduits for the passage of adsorbate molecules into the micro- and mesopores. Therefore, it is important to select activated carbon with the right pore distribution in practice based on the unique characteristics of the specific target water.

2.2.2.2 Surface chemistry

In graphites that have a highly ordered crystalline structure, the adsorption capacity is determined mainly by the dispersion component of the van der Walls forces. But the random ordering of the aromatic sheets in activated carbons causes a variation in the arrangement of electron clouds in the carbon skeleton and results in the creation of unpaired electrons and incompletely saturated valencies, which would undoubtedly influence the adsorption properties of activated carbons. The chemical groups found on an activated carbon surface are directly attributed to (a) the activated carbon precursors; (b) the method of activation; and (c) any additional treatment conditions.

Attempts have been made to identify and estimate the surface functional groups using several physical, chemical and physicochemical techniques, which include neutralization of bases, desorption of the oxide layer, potentiometric, thermometric, and radiometric titration, direct analysis by specific chemical reaction, polarography, infrared (IR) spectroscopy and X-ray photoelectron spectroscopy (XPS). As shown schematically in Figure 2.2, several nitrogen and oxygen species with quite different chemical behavior may

coexist on the surface of activated carbon. Among various surface functional groups, oxygen-containing structures are the best understood by now. However, the nitrogen functionalities in activated carbon surfaces are not very well understood.

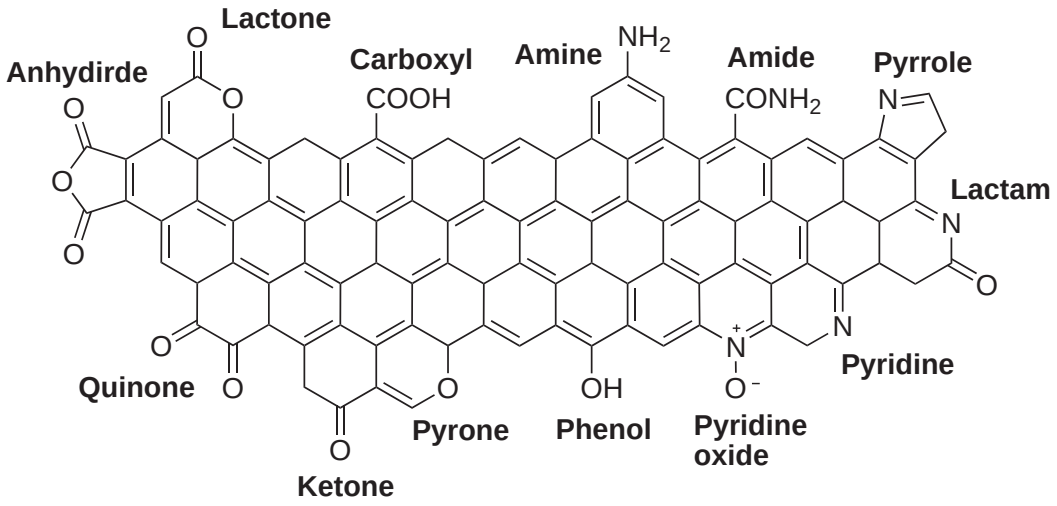

Figure 2.2: Nitrogen and oxygen functionalities in carbon materials (adopted from Li et al. (2009) and Arrigo et al. (2010))

2.2.2.2.1 pH of carbons and point of zero charge The pH of an aqueous slurry of carbons constitutes a useful indicator of the nature of the functionalities present on the carbon surface. In solution, Brönsted acidic groups of the carbon surface tend to donate their protons to water molecules and hence the surface becomes negatively charged. On the other hand, Lewis bases adsorb protons from solution, becoming positively charged. It is known that most of the oxygen-containing functionalities behave as Brönsted acids, donating protons to the aqueous media and being responsible for pH$<$ 7 of carbons. Thus, the different surface functionalities are responsible for the amphoteric nature of carbon, for the pH in aqueous solution, and for the surface charge. The American Society for Testing Materials (ASTM) has developed standard tests for measuring the pH of carbon backs and activated carbons in water.

The pH_{zpc} is defined as the pH where the net surface charge, resulting from the adsorption of the potential determining ions, H^+ and OH^-, is zero. Therefore, the pH_{zpc} can be considered also as the pH value below which the surface of the carbon particles in solution is, on average, positively charged, the converse being true for pH $<$ pH_{zpc}. It has been suggested that electrophoretic mobility measurements are only representative of the external surface charges of carbon particles in a solution (the internal surface charges cannot be measured by this method), whereas the pH_{zpc} varies in response to the net total (external and internal) surface charge of the particles.

2.2.2.2.2 Titration methods Titration with alkalies is one of the earliest and simplest methods used to determine the nature and amount of surface acidic groups on carbons. Boehm (1966) differentiated the acidic surface groups on oxidized charcoal and carbon black by selective neutralization technique, using bases of different strengths, namely $NaHCO_3$, Na_2CO_3, NaOH, and C_2H_5ONa (Boehm, 1966). The strongly acidic groups neutralized by $NaHCO_3$ but not by Na_2CO_3 were postulated as lactones. The weakly acidic group neutralized by NaOH but not by Na_2CO_3 was postulated as a group of phenols. The reaction with sodium ethoxide was not considered a true neutralization reaction because it did not involve an exchange of H^+ ions by Na^+ ions. The groups reacting with sodium ethoxide but not with sodium hydroxide were suggested to be carboxyls, which were created by the oxidation of the disorganized aliphatic carbon.

2.2.2.2.3 Thermal desorption methods This technique generally involves heating the carbon sample in vacuum or in an inert flowing carrier gas at a programmed heating rate (Vickerman & Gilmore, 2009). The oxygen-containing surface groups decompose into volatile gaseous products, which are then analyzed by conventional methods such as gravimetry, mass spectroscopy, gas chromatography, and IR spectroscopy. For instance, the carbon-oxygen surface groups are generally evolved as CO_2, CO, and water vapor, the amount of each gaseous species depending upon the nature of the carbon, its pretreatment, and the thermal desorption temperature. For example, CO_2 is evolved by the decomposition of carboxylic and lactomic groups in the temperature range 350 to 750 °C; CO by the decomposition of quinone and phenolic groups in the temperature range 500 to 950 °C; water vapor from the decomposition of carboxyls, phenols in the temperature range 200 to 600 °C.

2.2.2.2.4 X-Ray photoelectron spectroscopy X-ray photoelectron spectroscopy (XPS) is an ultrahigh vacuum technique (vacuum of the order of 10^{-9} Torr) used for surface characterization of solid and powder samples (Vickerman & Gilmore, 2009). Essentially, the technique measures the kinetic energy of electrons emitted from atoms after being irradiated by X-rays. The emitted electrons have measured kinetic energy (KE) given by:

$$KE = hv - BE - \phi_s \tag{2.1}$$

where hv is the energy of the photon, BE is the binding energy of the atomic orbital from which the electron originates, and ϕ_s is the spectrometer work function.

The penetration depth from which the photoelectron emerges is seldom more than 10 to 15 nm (i.e., about 10 to 20 atomic layers) from the surface, which makes the XPS

technique ideal for surface chemical analysis as well as for the study of adsorbed species. The technique has excellent sensitivity to submonolayer coverage and is able to detect all elements except hydrogen. In addition, it is useful for quantitative elemental analysis and can provide information on bonding from the measurement of chemical shift (Lahaye et al., 1999).

2.2.2.2.5 Infrared spectroscopy Infrared spectroscopy (IR) in its various forms is an important and forceful tool that can provide useful information about surface functional groups on carbons (Radovic, 2008). Special IR studies can also provide information regarding the molecular forces involved in the adsorption processes. The development of computerized Fourier-transform infrared spectroscopy (FTIR) has several advantages over conventional, dispersive IR spectroscopy. FTIR uses an interferometer in place of a grating or slits. This results in the availability of higher energy, of the order of 100 to 200 times over the dispersive system throughout the detector, enabling spectral information to be obtained for all frequencies at the same time. Coupled with an internally calibrated computer system to add a large number of interferograms, FTIR produces markedly superior spectra and can provide more precise information concerning the surface functional groups. The progressive changes in the surface chemistry of carbon materials upon modification treatments (oxidation, incorporation of nitrogen, annealing) and under different operating conditions detected by FTIR have been widely reported in the literature (Jansen & van Bekkum, 1994; Biniak et al., 1997; Chingombe et al., 2005; Seredych et al., 2008). Although the IR spectroscopy does not provide quantitative information about the carbon surface chemistry, it can identify the groups created or destroyed on the carbon surface upon modifying.

2.2.3 Modification of activated carbon surface

The polyaromatic sheets in activated carbons contain free radical structures or structures with unpaired electrons. These unpaired electrons are resonance stabilized and trapped during the carbonization process, due to the breaking of bonds at the edges of the polyaromatic sheets, and thus, they create edge carbon atoms (Radovic, 2008). These edge carbon atoms have unsaturated valencies and can, therefore, interact with heteroatoms such as oxygen, hydrogen, nitrogen, and sulfur, giving rise to different types of surface groups.

2.2.3.1 Activated carbon oxidation

Carbons are always associated with varying amount of chemisorbed oxygen unless special care is taken to eliminate the oxygen. Therefore, surface oxygen-groups are the most common type of functional groups found on activated carbon surfaces (Bandosz, 2006). In fact this combined oxygen has often been found to be the source of the property by which a carbon becomes useful or effective for some roles, and less useful for others.

Carbons have great tendency to extend this layer of chemisorbed oxygen, and many of their reactions arise because of this tendency. For example, carbons are capable of decomposing oxidizing gases such as ozone and oxides of nitrogen, chemisorbing oxygen. They also decompose aqueous solutions of silver salts, halogens, ferric chloride, potassium and ammonium persulfate, sodium hypochlorite, potassium permanganate, potassium dichromate, sodium thiosulfate, hydrogen peroxide, and nitric acid. In each case, there is chemisorption of oxygen and the formation of carbon-oxygen surface compounds. Carbons can also be oxidized by heat treatment in air, CO_2, or oxygen. The nature and amount of surface oxygen groups formed by different oxidative treatments depend upon the nature of the carbon surface and the history of its formation, its surface area, the nature of the oxidative treatment, and its temperature (Bansal & Goyal, 2005).

Moreno-Castilla et al. (2000) studied the changes in surface chemistry of several activated carbons oxidized by H_2O_2, $(NH_4)_2S_2O_8$ and HNO_3. The highest total oxygen content was obtained after the HNO_3 treatment and the lowest one after the $(NH_4)_2S_2O_8$ treatment. Both H_2O_2 and $(NH_4)_2S_2O_8$ treatments fixed most of the oxygen groups on the external surface of the carbon particles and the HNO_3 treatment on the internal surface. The techniques XPS and FTIR detected oxygen surface groups with single C−O bond, lactone, carboxyl, quinone or conjugated ketone and carboxyl-carbonate structures in all oxidized samples.

Mangun et al. (1999) oxidized activated carbon fibers (ACF) using both aqueous and nonaqueous treatments. It was found that as much as 29 wt % oxygen could be incorporated onto the pore surface in the form of phenolic hydroxyl, quinone and carboxylic acid groups. The average micropore size was typically affected very little by aqueous oxidation whereas the micropore volume and surface area decreased with such a treatment. In contrast, the micropore size and volume both increased with oxidation in air. Oxidation of ACFs produced surface chemistries in the pores that provide for enhanced adsorption of basic (ammonia) and polar (acetone) molecules at ambient and non-ambient temperatures. The adsorption capacity of the oxidized fibers for acetone was modestly better than the untreated ACFs while the adsorption capacity for ammonia increased up to 30 times compared to untreated ACFs.

Figueiredo et al. (1999) studied in detail the effect of different treatments on carbon surface. They employed techniques such as N_2 adsorption, X-ray photoelectron spectroscopy (XPS), temperature programmed desorption (TPD) and diffusion reflectance FTIR (DRIFTS) to characterize carbon surface properties obtained from gas/liquid oxidation and heat treatment in N_2. XPS and TPD results indicated that liquid phase oxidation (5 N HNO_3 or 10 M H_2O_2) increased carboxylic groups which evolved mostly as CO_2 during heat treatment; whereas gas phase oxidation (5% O_2) increased anhydride, lactone, phenol and carbonyl/quinone groups, which evolved as CO at high temperature by TPD. Also, liquid phase oxidation had almost no effect on pore structure. Gas phase oxidation increased pore width and volume. Heat treatment up to 600 °C removed carboxylic anhydrides and most of lactone, and some of phenol groups.

Porosity changes after nitric acid oxidation are different for carbons with different pore sizes. For mesoporous carbons, the response to oxidation can be quite complex. In the case of an ordered mesoporous carbon, the BET surface area and the porosity first increased and then decreased after nitric acid treatment (Li et al., 2006). The initial increase was considered to be the result of micropore generation. However, longer oxidation caused partial structural collapse, which resulted in the observed drop in surface area and pore volume. So, oxidation conditions must be carefully chosen to prevent excessive corrosion and structural breakdown of the carbon skeleton.

Oxidation increases carbon's acidity by creating acidic surface functional groups (carboxylic, phenolic groups et al.), and the carbon surface becomes more hydrophilic. The most obvious effect of oxidation is a decrease in pH_{pzc} (pH of point of zero charge). Decrease in pH_{pzc} means that oxidized carbon has a net negative surface charge at lower solution pH than untreated ones. The phenomenon is helpful for the adsorption of positively charged species while detrimental to anions or most organic compounds.

2.2.3.2 Thermochemical treatment by NH_3

The focus of this research is on surface modification of carbon to improve its adsorption for perchlorate. The study of anion adsorption on activated carbons is less advanced compared with adsorption of cations on activated carbons, because common activated carbon contains many oxygen functionalities and negatively charged sites. The preparation of carbons with positively charged surfaces is of great interest in perchlorate removal. Treatment with ammonia has been shown to be effective way to introduce such active sites (Chen et al., 2005a).

As opposed to oxygen functionalities, which are formed spontaneously on carbon

surfaces by contact with air, the amount of nitrogen in carbon materials is negligible and thus the carbon-nitrogen complexes are insignificant (Ayala et al., 2010). Thus, nitrogen functional groups usually exist in the carbon matrix as a consequence of the nitrogen presence in the precursor. However, nitrogen can be introduced in the carbon matrix by two methods: reaction with nitrogen containing reagents (i.e. ammonia, urea, melamine, HCN) or preparation of a carbon from a nitrogen-containing precursor (i.e., carbazole, nitrogen enriched polymers, acridine). In this context, much effort has been done on this subject in the last decade (Jansen & van Bekkum, 1994; Stanczyk et al., 1995; Menendez et al., 1996; El-Sayed & Bandosz, 2005; Pietrzak et al., 2007; Perez-Cadenas et al., 2009; Wang et al., 2010).

Bansal & Goyal (2005) found that when an oxidized carbon was heated with dry ammonia, nitrogen groups were formed on the carbon surface. At low temperature the fixation of nitrogen was equivalent to the number of acid oxygen groups and was attributed to the formation of ammonium salts. However, at high-temperature treatment a substitution of the hydroxyl groups by amino groups was postulated. Stohr et al. (1991) employed XPS to study the surface groups after carbons were treated with ammonia at 600-900 °C for 4 hours. XPS showed two N1s signals for ammonia treated carbon with binding energy of 401-400 ev and 399-398 ev, which they assigned to be amine groups and nitrile and/or pyridine-like nitrogen respectively. Heat treatment in N_2 and H_2 at 700 and 900 °C decreased the nitrogen content. The carbon was gasified in the reaction with NH_3 at 900 °C leading to an increase of the pore volume in micropore range. Carboxylic, hydroxyl and ether-like oxygen reacted with NH_3 leading to amide, nitrile, amine and pyridine- or acridine- like nitrogen created on the carbon surface.

Mangun et al. (2001) studied a series of ACFs and ammonia-treated ACFs. An apparent increase in N-content was observed after ACFs were treated in ammonia for 10-60 min at 500 to 800 °C. The increase in nitrogen was due to the addition of groups at the carbon edge sites where they directly affected adsorption properties. The types of groups present were analyzed by FTIR, XPS and TPD. They suggested that 500 °C treatment yields amide, aromatic amine and nitrile groups, whereas higher temperatures resulted in formation of aromatic amines and pyridine.

Xie et al. (2000) conducted a study on the microcalorimetry of acid and ammonia pretreated activated carbon as a probe of acid/base on carbon surfaces. Combined with techniques such as Boehm titration, pH_{zpc} and TPD, they concluded that the largest amount of ammonia was incorporated to the carbon at 400 °C while the corresponding pH_{zpc} values increased monotonically with the temperature of treatment. It was further pointed out that at high temperature, ammonia treatment was able to remove oxygen groups and in the process increased unsaturated edge sites. But, if the temperature was

too high, the previously created active carbon edge was gasified.

Nitrogen functional groups were also found to show transformation under treatment at different temperatures. Stanczyk et al. (1995) studied the influence of carbonization temperature on chars containing nitrogen groups, such as pyrrole, pyridine, amino and cyano groups. Carbonization was carried out in a fixed bed reactor in an argon flow at 460, 600 and 800 °C, respectively. Amount of N carbonized at 460 °C depended on the type of precursors and it decreased as the carbonization temperature increased. N/C was similar for 460 °C and 600 °C and was higher than that from 800 °C. The transformation of nitrogen functionalities is complicated. At low temperature, pyridine and pyrrole structures transformed into each other (depending on the precursor) while they transformed into more stable quaternary N at higher temperatures (800 °C). XPS studies on nitrogen functionalities in coals indicated that pyrrolic and pyridinic groups are the main constituents. There are also quaternary and nitro/nitroso groups present. The exact structure of quaternary may be protonated pyridinic-N as described by some researchers (Jansen & van Bekkum, 1994). When coals were subjected to pyrolysis, nitrogen functionality distribution changed with the severity of pyrolysis. Under severe pyrolysis, the final distribution was not relevant to the original material. Pyrrolic-N was found stable at T as high as 600 °C. Above that, it converted gradually into pyridinic-N or quaternary-N.

Li et al. (2009) prepared bulk quantities of N-doped, reduced graphene oxide (GO) sheets through thermal annealing of GO in ammonia. XPS study of GO sheets annealed at various reaction temperatures revealed that N-doping occurred at a temperature as low as 300 °C, while the highest doping level of $\sim 5\%$ N was achieved at 500 °C. Oxygen groups such as carboxylic, carbonyl, and lactone groups were suggested to be essential for reactions between graphene and NH_3 for C−N bond formation. For different graphene samples with varying degrees of oxidation, the degree of reaction with ammonia and N-doping depended on the amounts of these oxygen functional groups at the defect and edge sites of graphene.

Arrigo et al. (2010) studied the influence of the temperature of the amination treatment with ammonia on the population of nitrogen and oxygen species and the impact of functionalization on the electronic and surface properties of the carbon materials (carbon nanofibers). Using synchrotron based XPS, it was found that at 473 K nitrogen moieties were introduced as consequence of the reaction of carboxylic acid sites. As the functionalization temperature increased, pyridine-like and pyrrole-like species increased, leading to a surface with hydrophobic character.

2.3 State of the art of perchlorate removal using N-alkyl quaternized activated carbon

Perchlorate (ClO_4^-) has been widely used as a rocket propellent and in munitions in the United States and abroad, and improper disposal of perchlorate-containing materials has resulted in a significant new threat to groundwater and drinking water supplies. Because perchlorate ions are highly soluble and kinetically inert in dilute aqueous solutions, they cannot be effectively removed from water by conventional carbon filtration or by chemical reduction.

Activated carbon adsorption is a cost effective technique for removal of organic contaminants and has been widely used for more than 50 years to treat public water supplies. The removal capacity of virgin activated carbon for perchlorate was found to be low due to the oxygen functionality and negatively charged surfaces of the carbon. Nonetheless, activated carbon does offer the advantage of having large surface area and after appropriate surface modifications, it has been shown to be competitive for perchlorate removal.

Activated carbon is a complex and heterogeneous material with unique adsorption characteristics. The main features that give the material these characteristics are its porous structure, surface area and surface properties. High specific surface area and large micropore volume (especially micropores with widths that are one to ten times the dimensions of the adsorbate) have long been proven to be helpful for adsorption. On the other hand, more work still needs to be done to understand the surface chemistry effects on carbon performance.

Present research has focused on modifying the carbon surface with N-alkyl quaternized functionality so that the carbon achieves higher adsorption capacity for perchlorate from natural water, without undermining the pore structure that is beneficial to the perchlorate adsorption. It is expected that armed with a relatively full understanding of the factors affecting perchlorate adsorption, nevertheless should be able to achieve a more favorable method of tailoring carbon to remove perchlorate.

Chapter 3

Statement of goals; objectives and hypotheses

3.1 Goal statement

Perchlorate is an oxyanion with unique properties that make it commercially useful as an oxidizing agent in rocket fuels, fireworks, and flares. However, widespread commercial use has lead to the presence of perchlorate in the ground and surface water of 26 states, especially in the Southwest U.S. (Urbansky, 1998). Perchlorate is very soluble, kinetically slow-reacting, and difficult to chemically reduce or precipitate, which enables it to be environmentally persistent and untreatable with most standard water treatment methods. Conventional commercial activated carbon has typically been used to remove organic contaminants from water due to its hydrophobic surface and extensive pore structure. Conventional activated carbon, however, is unable to effectively remove inorganic ions, such as perchlorate. The need for cost effective treatment of perchlorate has spurred this research.

The main goal of the research is to remove perchlorate from ground water using activated carbon tailored with pyridinium functional groups.

3.2 Objectives

Objectives of this research are:

1. To prepare nitrogen-tailored activated carbon with N-alkyl quaternized functional-

ity and high mesopore volume through choosing proper raw material and optimizing nitric acid pretreatment, NH_3 thermal treatment and quaternization reaction.

2. To introduce pyridine type nitrogens on the activated carbon surface through thermal treatment in NH_3.

3. To transform pyridine type nitrogen to N-alkyl pyridinium through quaternization reactions.

4. To characterize the surface chemistry and pore structure of N-alkyl pyridinium tailored carbon.

5. To demonstrate the efficiency of the functionalized activated carbon in treating perchlorate contaminated water.

3.3 Hypotheses

Based on the above goal and objectives, the following hypotheses are proposed:

1. The nitrogen content of the ammonia tailored carbon is positively correlated to the oxygen content of the nitric acid treated carbon.

2. Tailoring with N-alkyl pyridinium functional groups would enhance the perchlorate adsorption capacity.

Chapter 4

Methodology

4.1 Introduction

This section presents an account of experiments and activities for carrying out the specific objectives and hypotheses testing. A general overview of the methodology is given and is followed by a methodology flowchart (Figure 4.2). The flowchart shows step-wise procedures and decision making steps involved in the research.

4.2 General overview of experimental phases

The research activities were divided into three main phases: I, II and III (Figure 4.2). Phase I involves sample preparation of the nitrogen tailored activated carbon. The sample preparation included three steps: nitric acid oxidation, thermal treatment in ammonia and the quaternization reaction, relating to objective 1, 2 and 3.

The aim of nitric acid treatment was to introduce different oxygen functional groups, such as carbonyl, carboxyl, and phenol groups, onto the surface of the carbon (Figure 4.1), while maintaining the pore structure of the carbon. At different reaction temperatures, different amounts and types of oxygen functionality are generated, however, pore structures collapse at higher temperature. So, in this step, we use reaction temperature as a optimization factor.

The aim of thermal treatment in ammonia was to (a) open up extensive microporosity and mesoporosity throughout the nitric acid treated carbon, and (b) cause available edge sites to become reactive by breaking C−O bonds (Figure 4.1). This step is re-

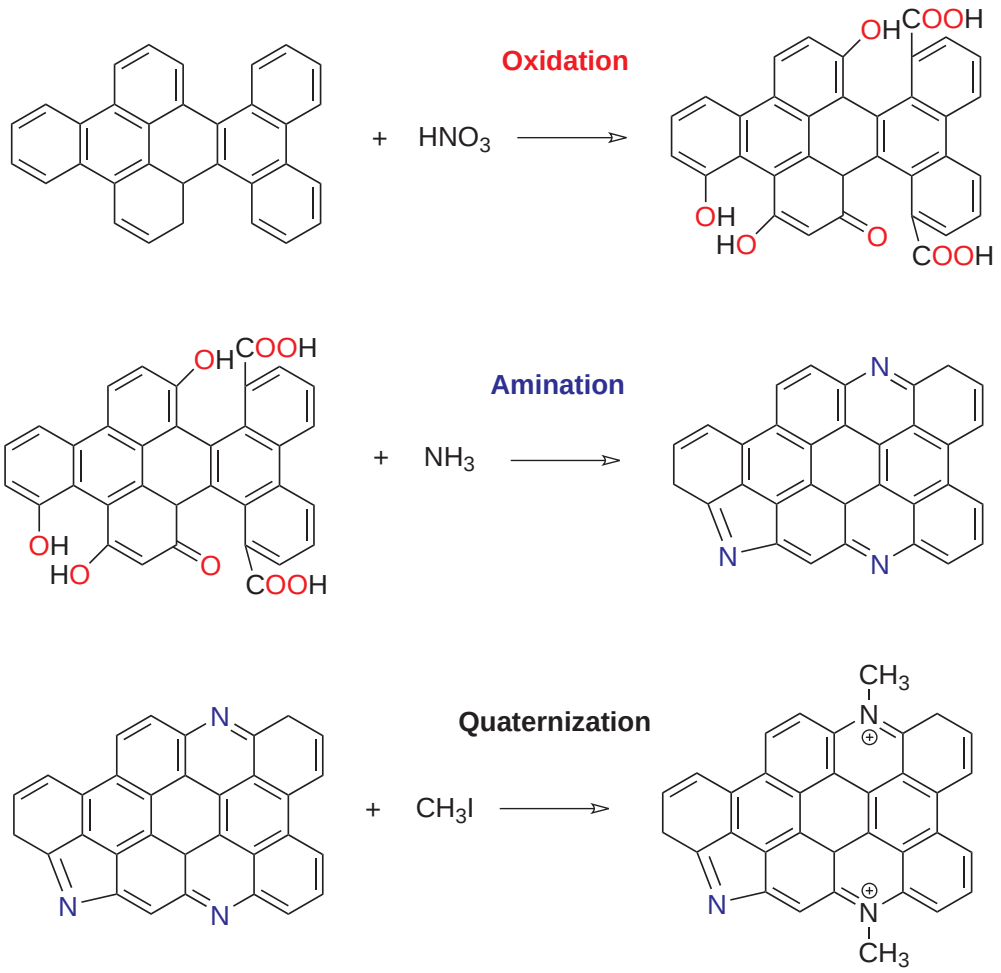

Figure 4.1: Schematic diagram depicting possible reactions during nitric acid oxidation, amination and quaternization.

lated to hypothesis 2. We anticipate that in a radiant-heat (i.e. conventional) furnace, C−O bonds will be broken over the temperature range of 200-800 °C, while pyridine functionality will form following ammonia gas exposure at 500-800 °C. With this as our perspective, we conducted thermal treatments in a cylindrical glass fluidized bed reactor that employ an array of temperatures from 450-800 °C, an array of gas environments and gas sequences including N_2, NH_3, CO_2, H_2O, etc., and an array of gas flow rates from 0 to 100 ml/min. The ammonia tailoring step is the key step to introduce the nitrogen functionality. So the ammonia flow rate and the ammonia reaction temperature were optimized to maximize pyridine type nitrogen on the carbon surface.

The next tailoring step was to convert the pyridine edge sites to alkyl pyridinium edge sites (Figure 4.1). The alkyl pyridinium is the preferred functional group, because it has a high affinity for perchlorate and nitrate. To achieve quaternization, we employed different alkyl halide reactants: methyl iodide, 1-bromopropane, 1-bromohexane and

1-bromohexadecane.

The surface chemistry and pore structure of samples from each step were characterized (phase II) and the reaction conditions were optimized. In this phase, the pore volume distribution and specific surface area of GACs were determined by adsorption of argon vapor; the surface chemistry was characterized by XPS.

In phase III, the final products were tested via perchlorate adsorption tests. This is related to objective 5 and hypotheses 2. Isotherm tests were used to determine the adsorption capacity of the carbon sample. Rapid small scale column tests (RSSCTs) were designed to simulate full-scale filter-bed adsorbers that provide an empty-bed contact time (EBCT) of 7.5 minutes, which is fairly typical.

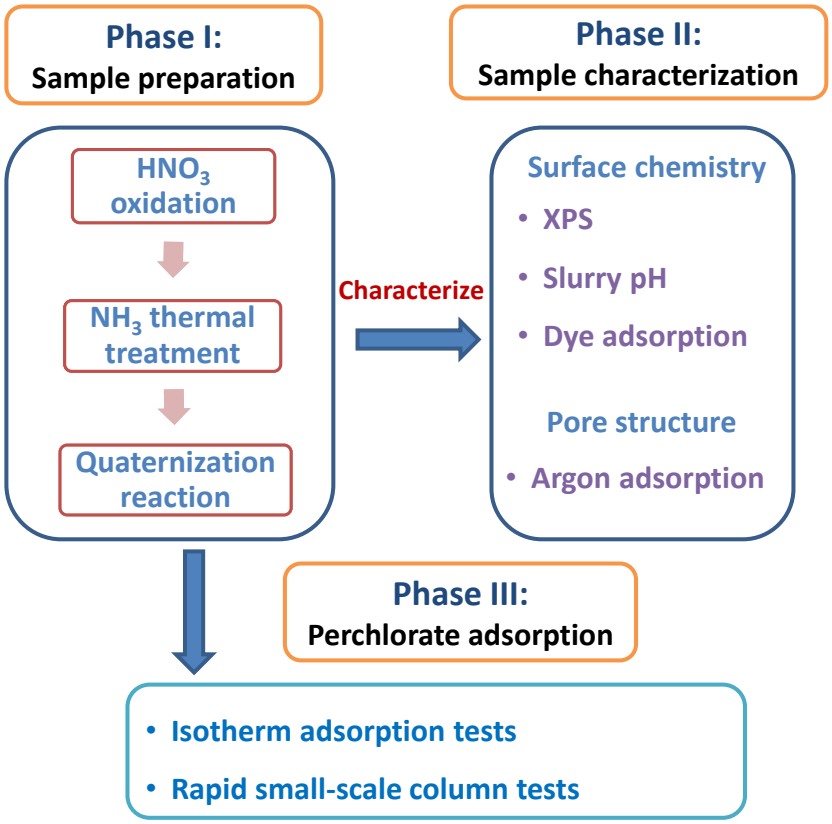

Figure 4.2: Schematic for preparation and characterization of N-alkyl quaternized activated carbon and testing perchlorate removal capacity.

4.3 Sample preparation

4.3.1 Granular activated carbon

GACs used in this study are listed in Table 4.1. GACs were ground and sieved to U.S. mesh 200 × 400 (75-37 μm). They were then washed with deionized-distilled water to remove fines, and dried at 105 °C overnight to remove moisture. The carbon samples were stored in desiccator under vacuum until use.

Table 4.1: Typical characteristics of activated carbons.

Carbon type	**Abbreviation**	**Base material**	**BET area (m^2/g)**	**Brief description**
AquaCarb 1240C	AC1240C	coconut shell	859	Steam & CO_2 activated
UltraCarb 1240	UC1240	bituminous coal	967	Steam & CO_2 activated
Gran C	GC	oak wood	1460	H_3PO_4 activated
Nuchar RGC	RGC	hard wood	1545	H_3PO_4 & steam activated

4.3.2 Oxidation by nitric acid

Carbon oxidation was conducted by mixing 10 g of the carbon with 100 mL of nitric acid solution (7.9 N). The carbon and nitric acid mixture were held and constantly stirred for 6 h at different temperature (20, 50, 80, 95, 105 °C). The oxidized activated carbon samples were washed until the pH of the filtrate reached almost neutral. The washed samples were dried at 105 °C overnight and stored in desiccator under vacuum.

The aim of this step was to increase the oxygen content and maintain the pore structure. The content and type of oxygen was analyzed by XPS and the pore structure was measured by argon adsorption.

4.3.3 Thermal treatment by ammonia

Ammonia tailoring was carried out using a cylindrical glass fluidized bed reactor in a 3210 furnace/oven manufactured by Applied Test Systems, Inc. (Butler, PA). Flow meter and flow regulators were calibrated and used to set flow rates. The furnace was heated to a desired temperature (optimization factors: 450, 600, 700, 800 °C) in mixture atmosphere of nitrogen and ammonia (anhydrous, min. purity 99.99%). The total flow rate of nitrogen and ammonia was controlled at 100 ml/min to maintain the fluidized condition. The ammonia flow rate was held at desired value (0, 1, 2, 5, 10, 20, 40, 60 ml/(min · g)). The carbon samples were treated in ammonia for a predetermined time

(30 min) at constant temperature and then cooled to room temperature under a nitrogen atmosphere. The samples were then washed until constant pH, dried in a 105 °C oven, and stored in desiccator under vacuum until use.

The aim of this step was to introduce the pyridine nitrogen and maintain the pore structure. The content and type of nitrogen was analyzed by XPS and the pore structure was measured by argon adsorption.

4.3.3.1 Quaternization reaction

Pyridinic nitrogen at the accessible carbon surface was transformed to quaternary nitrogen by reacting the carbon with alkyl halide reactants (methyl iodide, 1-bromopropane, 1-bromohexane and 1-bromohexadecane). The carbon sample (1 g) was suspended in a 50 mL solution of alkyl halide reactants (15 mL) in methanol and stirred at 45 °C for 6 h. Then the mixture was filtered through 1 μm nylon membrane and the residue was washed with ethanol four times. Due to the light sensitivity of alkyl halide reactants, samples were reacted and stored in amber glass vials covered with the aluminum foil.

4.4 Sample characterization

4.4.1 Pore volume distribution and specific surface area determination

To analyze pore structure, both a Micromeritics Accelerated Surface Area and Porosimetry analyzer (ASAP) 2000 and 2010 were used. Prior to preparation for analysis, all wet activated carbon samples were oven-dried at temperatures between 90-150 °C for at least 10 hours. On average, 500 mg of dried carbon sample was weighed for analysis. This was referred to as “wet” weight, since the carbon samples were not yet rigorously heated and degassed by the ASAP unit. Empty tubes were weighed three times prior to and after being filled with carbon sample to ensure accuracy. Carbon samples were then heated at 105 °C and degassed to 0.009 Torr. To conduct a pore volume analysis, successfully heated and degassed carbon samples were dosed to atmospheric pressure with gaseous Argon, cooled to about 20 °C, then removed from the ASAP analyzer and weighed three times. Subtracting the initial, empty weight of the tube from the weight of the degassed then dosed carbon sample, yielded a “dry” sample weight, which was required to conduct a pore volume distribution. With each incremental pressure increase, the number of gas molecules adsorbed on the surface increases. The pressure at which adsorption equilibrium occurs was measured and the universal gas law was applied to determine the quantity of gas adsorbed.

As adsorption proceeded, the thickness of the adsorbed film increased. Any micropores in the surface were quickly filled, then the free surface became completely covered, and finally larger pores were filled. The process would continue to the point of bulk condensation of the analysis gas. Then, the desorption process would begin in which pressure systematically is reduced resulting in liberation of the adsorbed molecules. As with the adsorption process, the changing quantity of gas on the solid surface was quantified. These two sets of data described the adsorption and desorption isotherms. Analysis of the isotherms yielded information about the surface characteristics of the material (Moore et al., 2003; Chen et al., 2005a).

Requiring a significantly shorter amount of time, single point adsorption analysis (cm^3 of gaseous argon/g of GAC) was used for screening, before conducting a full pore volume distribution. Consequently, the single point adsorption analysis became the primary mechanism that was initially used to compare pore structure between samples. These analysis depicted the volume of argon (as a gas at standard condition for temperature and pressure) adsorbed into the carbon sample, in which the sample had been degassed down to 6.6×10^{-6} atm, placed in a liquid argon bath (-185.7 °C),and then loaded with argon gas up to 9.5×10^{-3} atm. At this pressure and temperature, the density functional theory (DFT) theory dictates that argon condensation will occur in slit pores up to a 10-12 Å width (Rangel-Mendez & Cannon, 2005). For the Micromeritics 2000 and 2010 ASAP analyzers, full pore volume distributions required approximately between 72 and 96 hours to complete. A single point adsorption analysis, however, could be completed in 1-12 hours, since only one (low) partial pressure equilibrium point was analyzed (Rangel-Mendez & Cannon, 2005). This work was done by Tim Byrne and Colin Cash.

4.4.2 Dye adsorption

Methylene blue is a cationic dye with the critical pore diameter to be 15.2 Å which corresponds to the upper portion of the micropore region. Methylene blue dye adsorption tests are used to rather rapidly characterize the extent of larger micropore volume and negative surface charge of sample carbons (Pittman et al., 1997).

Methylene Blue Dye Powder with a total dye content of 82% was obtained from Fisher Scientific Company (Fair Lawn, NJ). The dye was dried in a vacuum oven overnight to determine its hydrate content and stock solutions were prepared accordingly. Stock dye was created at 200 mg/L and buffered to pH 2.6 using 5% Acetic Acid, Glacial (J.T. Baker, Phillipsburg, NJ). Methylene blue adsorption tests were carried out in triplicate using 150 mL of 200 mg/L dye solution with 60 mg of carbon adsorbent. Dye solutions

were shaken for 20 hours at 30 °C on an orbital shaker. The supernatant dye was then removed by centrifugation at 5000 rpm for 20 min. Samples were then diluted within the range of Beers law standard calibration (1-10 mg/L) and measured using a Shimazdu 1601 UV/Vis spectrophotometer at a wavelength of 620 nm. This work was done by Tim Byrne.

4.4.3 Slurry pH

Slurry pH is an indication of the aggregate acidity of the carbon surface. A low slurry pH indicates a surface with functionalities having low pKa values (i.e. oxidized functional groups such as lactones and carboxyl groups). In contrast, a high slurry pH could be indicative of nitrogen functionality, such as quaternary ammonium, pyridinium, and amines (Arrigo et al., 2010).

The slurry pH method: 1.75 grams of sample carbon was place in 17.5 mL of DI water; and the mixture was placed into a sealed 4 dram (20 ml total volume) glass vial. After the addition of glass beads, the vials were placed on a shaker table for 24 hours at 30 °C to "equilibrate". The equilibrium pH was measured after minimal contact with the atmosphere. This work was done by Tim Byrne.

4.4.4 X-ray photoelectron spectroscopy

X-ray photoelectron spectroscopy (XPS) is an ultrahigh vacuum technique (vacuum of the order of 10^{-9} Torr) used for surface characterization of solid and powder samples. The technique has excellent sensitivity to submonolayer coverage and the ability to detect all elements except hydrogen. Normally a quick survey scan was completed for each sample to identify the elements present with a high generation energy and short dwell time. Once the elemental composition had been determined, narrower detail scans of selected peaks were collected for quantification and chemical state information with a low generation energy and long dwell time. XPS was performed with a Kratos Analytical Axis Ultra XPS (Kratos Analytical, Manchester, U.K.). Ground carbon samples could be directly used by XPS. XPS is particularly suited for the recognition of the surface species on carbon material as the measured BE shift is sensitive to the electronic structure of the photoemitting atom (Arrigo et al., 2010). XPS data provide information on the surface chemical nature of the functional groups through analysis of the C1s, N1s and O1s spectra.

4.5 Perchlorate adsorption tests

4.5.1 Water sources

Penn State University tap water and groundwater taken from Penn State Well 17 spiked with 30 ppb perchlorate were used for RSSCTs experiments. Standard and stock perchlorate solutions were prepared by dissolving ACS grade solid anhydrous sodium perchlorate (EM Science, Gibbstown, NJ) in DI water.

Deionized-distilled (DI) water used for preparing stock solutions and standards was treated by a Millipore Milli-Q Academic system with conductivity equal or exceeding 18.1 MΩ/cm^2.

4.5.2 Perchlorate analysis

Perchlorate concentrations were measured using a Dionex DX 500 Ion Chromotography unit. The DX 500 was equipped with a 4-mm AS16 column, a 4-mm AG16 guard column, a 4-mm ASRS 300 ultra suppressor, and a DS3 detection stabilizer. An eluent concentration of 25 mM NaOH was used. Method detection limit (MDL) of perchlorate was around 5 ppb. A 25 μL loop was used for perchlorate concentration in the range of ppm. Part of this work was done by Tim Byrne, Colin Cash and Pin hou.

4.5.3 Isotherm adsorption tests

Isotherm adsorption tests were conducted using a 30 mg of carbon sample in 22.5 ml bottles of 30 ppb, 120.3 ppb, 350 ppb, 1.2 ppm, 4 ppm, and 13.5 ppm starting concentrations of perchlorate in DI water. The bottles were mixed at room temperature on a rotary shaker (20 rpm) for 24 h, which was determined to be a sufficient equilibrium time. After reaching the predetermined equilibrium time, the samples were filtered through 0.45 μm nylon filters to separate carbon particles, and the perchlorate concentration was measured by ion chromatography.

The amount of the perchlorate adsorbed (mg) per unit mass of carbon samples, q_e, was obtained by using the equation

$$q_e = \frac{(C_i - C_e)V}{M} \tag{4.1}$$

where C_i and C_e are initial and equilibrium concentrations in mg/L, M is the dry mass of carbon in grams, and V is volume of solution in liters. This work was done by Tim

Byrne and Pin hou.

4.5.4 Rapid small-scale column tests

To conduct Rapid Small-Scale Column Tests (RSSCTs), several plastic columns were used. These plastic columns featured a narrow, circular shaft that was bored cleanly down the vertical axis of the column. The top and bottom of the column were threaded for attaching influent and effluent lines. The column measure 0.36 cm in diameter, and 8.2 cm long; yielding a 0.8 mL bed volume (BV).

It was assumed that proportional diffusivity applies to these RSSCTs. The appropriate flow rate for the RSSCTs was determined using the following equation for Empty Bed Contact Time (EBCT) for constant diffusivity:

$$\frac{\mathrm{EBCT_{SC}}}{\mathrm{EBCT_{LC}}} = \frac{d_{\mathrm{SC}}}{d_{\mathrm{LC}}} \tag{4.2}$$

where SC: small column, LC: large column and d is carbon grain diameter.

Since the carbon sample was ground, washed and sieved to U.S. mesh 200×400, the average grain size for the small column (d_{SC}) was 56 μm, and the average grain size for the large column (d_{LC}) was 1.06 mm (US mesh 12×40). Additionally, the $\mathrm{EBCT_{LC}}$ was assumed to be 20 minutes. This gived an $\mathrm{EBCT_{SC}}$ of 1.05 minutes. Therefore, the desired flow rate was indicated by $\mathrm{BV/EBCT_{SC}}$; which, in this case, was 0.8 mL /1.05 min = 0.76 mL/min.

The procedure for RSSCTs began by packing one end of the column with glass wool, filling the column with carbon sample, then packing the remaining end. A cleaned straight-tip hemostat was used to tightly pack the glass wool, and as the sample was added, the column was gently tapped on a hard surface, to encourage tight packing of the carbon grains. The packed columns were attached to a Waters HPLC 510 pump, which have been washed with DI water. The lines connecting the HPLC pump to the column were also previously washed with DI water. After attachment to the HPLC pump, the filled columns were subjected to a cleaning and/or soaking process. Once a RSSCTs was initiated, samples were collected regularly, in 15 mL scintillation vials. By recording the empty weight of the vials and collection time, flow rate was established and maintained. Part of this work was done by Tim Byrne, Colin Cash and Pin hou.

Chapter 5

Experimental Results and Discussion

5.1 X-ray Photoelectron Spectroscopy study of active carbons

X-ray photoelectron spectroscopy (XPS) is an ultrahigh vacuum technique (vacuum of the order of 10^{-9} Torr) used for surface characterization of solid and powder samples. The technique has excellent sensitivity to submonolayer coverage and the ability to detect all elements except hydrogen. Development of XPS is essential for a more complete understanding of nitrogen chemistry of activated carbon (Bandosz, 2006).

In X-ray photoelectron spectroscopy (XPS), photon electrons are excited by X-ray irradiation and leave the atoms. Their binding energy is derived from the measured kinetic energies. The binding energy depends on the atomic species but is also affected by the nuclear charge, which is lowered or raised by bonding of the atom to more electronegative or electropositive atoms. The differences in binding energy (i.e., chemical shift) for various binding states are quite small compared to the line width, especially with electronegative elements such as oxygen or nitrogen. Thus, it is rare when individual subpeaks are completely separated in an experimental spectrum. This requires the use of peak-fitting procedures to resolve the desired peak parameters. Parameters used in such procedures include the background, peak shape (e.g., Gaussian, Lorenzian, asymmetric, or mixtures thereof), peak position, peak height, and peak width. For spectra containing severely overlapping peaks, the results obtained from peak fitting depend on the starting parameters chosen (Estrade-Szwarckopf, 2004). Appropriate purified standard specimens (model compounds) can be used to get these parameters.

5.1.1 Separation and identification of the different types of nitrogen 1s

Here, XPS is used to monitor the functionalization of activated carbon. Specifically, we analyze the oxidation, then amination, and ultimately the conversion the to quaternary nitrogen cations.

5.1.1.1 Pyridinic (N6)

According to the literature, binding energy of the pyridinic-type nitrogen N1s lies between 398.3 and 399.4 eV. The "pyridinic" N-atom is sp^2-hybridized, with the ion-pair electrons in the sp^2 hybrid orbital that does not participate in the π-system. The non-bonding (sp^2) electron is therefore easier to ionize than an electron in a π-system and hence appears in the XPS spectrum at lower BE. When the component peak corresponding to pyridinic nitrogen is individualized by curve-fitting of a complex N1s envelope, the accuracy for the position of this component is dependent upon the relative intensity of the N1s peak. For nitrogen tailored activated carbon with low nitrogen content, the uncertainty may be significant.

5.1.1.2 Pyrrolic (N5)

Another major functional form of nitrogen bound in carbonaceous materials is pyrrolic nitrogen. The values of the energy difference between the pyridinic nitrogen component and the pyrrolic-type component are equal to 1.4 ± 0.2 eV. The term "pyrrolic" is used to refer to N atoms with two p-electrons on the π system although not necessarily in a five-member ring as in pyrrole (Casanovas et al., 1996). The N1s peaks of pyrrolic nitrogen include pyrrole and pyridone functionalities and are generally of a weak intensity, which increases the uncertainties. The pyridone species is the tautomeric form of a lactam and is represented as a pyridine species with hydroxyl group in the α-position to the N atom in the aromatic ring. Through analogy with the BE of model compounds, there are several possible species, all of which have nearly the same BE: amino groups attached to aromatic rings, amide groups, and nitroso groups (Arrigo et al., 2010). In addition, in carbon samples, besides the pyrrolic and pyridinic nitrogen, a significant proportion of the heterocyclic nitrogen is pyridonic. The binding energy of pyridonic N is close to the one of pyrrolic nitrogen; and the two therefore cannot be distinguished from one another by XPS.

Table 5.1: Binding energies of N 1s relative to C 1s at 284.8 eV for a number of model compounds

Compounds	**Peak position (eV)**	**Nitrogen type**	**Ref**
Phenanthridine	398.5	Pyridine	(Bartle et al., 1987)
Phenazine	398.7	Pyridine	(Bartle et al., 1987)
Poly(2-vinylpyridine)	398.8	Pyridine	(Kelemen et al., 1994)
3-Hydroxypyridine	398.8	Pyridine	(Kelemen et al., 1994)
Norharman	398.8	Pyridine	(Kelemen et al., 1994)
PIB amine	399.1	Amine	(Kelemen et al., 1994)
1-Aminopyrene	399.2	Amine	(Bartle et al., 1987)
1-Aminopyrene	399.3	Amine	(Kelemen et al., 1994)
l-Aminofluorene	399.2	Amine	(Bartle et al., 1987)
Norharman	400.1	Pyrrole	(Kelemen et al., 1994)
Carbazole	400.1	Pyrrole	(Bartle et al., 1987)
2-Hydroxycarabazole	400.2	Pyrrole	(Kelemen et al., 1994)
Dibenzocarbazole	400.2	Pyrrole	(Kelemen et al., 1994)
1-Hydroxyquinoline	400.3	Pyrrole	(Kelemen et al., 1994)
1-Methyl-4-pentadecyl 2(1H)-quinolone	400.4	Pyrrole	(Kelemen et al., 1994)
6-(2,2-diphenyl-2-hydroxylethyl)-2(1H)-pyridone	400.5	Pyrrole	(Kelemen et al., 1994)
Quaternarized phenanthridine	401.2	Quaternary	(Bartle et al., 1987)
1-Ethyl-4-methoxypyridinum iodide	401.3	Quaternary	(Kelemen et al., 1994)
Pyridinium 3-nitrobenzenesulfonate	401.4	Quaternary	(Kelemen et al., 1994)
3-Hydroxypyridine N-oxide	403	N-oxid	(Kelemen et al., 1994)
9-Hydroxy-3-nitroflourene	405.3	Nitro	(Kelemen et al., 1994)
Pyridinium 3-nitrobenzenesulfonate (nitro)	405.8	Nitro	(Kelemen et al., 1994)
1-Nitropyrene	405.9	Nitro	(Kelemen et al., 1994)
1-Nitropyrene	406	Nitro	(Bartle et al., 1987)

5.1.1.3 Quaternary (NQ)

In nitrogen-doped carbon samples, many authors identify a third component that is positively shifted between 2.6 ± 0.1 eV with respect to the pyridinic component. It is attributed to "quaternary" nitrogen. Actually, according to the sample examined, the "quaternary nitrogen" component corresponds to several different forms of heterocyclic nitrogen. Pyridinium-type N, usually quaternarized from pyridine, corresponds to real quaternary nitrogen. Pyridinic nitrogen hydrogen bonded to adjacent phenolic $-$OH or $-$COOH also contributes to quaternary nitrogen. Pyridinic-type nitrogen incorporated to the polyaromatic sheets is also a source of quaternary nitrogen, which is also assigned to the so-called substitutional "graphitic" nitrogen. Substitutional N refers to N substituting a C atom in the graphitic structure, in which the nitrogen forms three σ-bonds with neighboring C or H atoms and contributes two electrons to the π-system.

5.1.1.4 Oxidized nitrogen (NOx)

It is generally accepted that, in the N1s XPS spectrum, oxidized forms of nitrogen show BE above 402 eV (Table 5.1). The component corresponding to nitro-type nitrogen ($-NO_2$) is shifted by 6.5 to 7.0 eV with respect to the pyridinic nitrogen, while nitro-functionalities are shifted by 4.5. Table 5.1 shows the binding energies for a range of model compounds containing the nitrogen functional groups. On the basis of these literature reports, the N6 peak at lower binding energy can be mainly assigned to pyridine and nitrile groups, and the N5 peak to amine, amide, lactam and pyrrole groups. The NQ component can be assigned to highly coordinated nitrogen atoms bound to three C atoms in the bulk of a graphene layer and, finally, the NOx peak to the pyridine-N-oxide, which gives a peak above 405.0 eV.

Two kinds of standards have been used herein: a compound representing pyridine structure (N6) (poly(2-vinylpyridine)) and another representative of pyridinium salts (NQ). In order to make these standards, pyridinium salts with different alkyl chain lengths were synthesized through alkylation reactions between pyridine and corresponding alkyl halide in our lab.

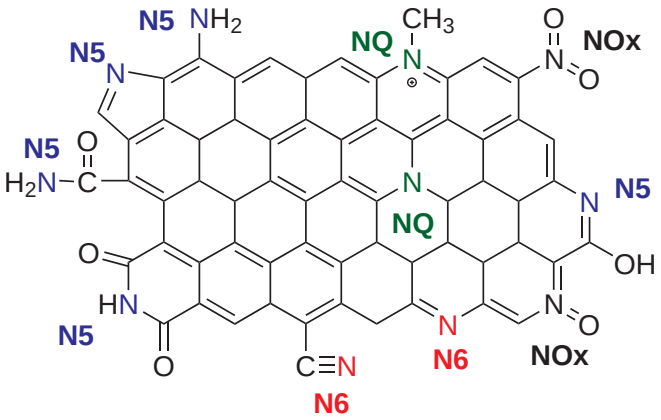

Figure 5.1: Schematic structure of typical nitrogen functionality for XPS curve fitting

The curve fitting results of poly(2-vinylpyridine) and pyridinium salts are presented in Table 5.2. The N1s envelopes were curve-fitted using mixed asymmetric Gaussian-Lorentzian component profiles after subtraction of a Shirley background using the CasaXPS software (version 2.3.12). In all electron spectra of aromatic ring systems, strong satellite lines were observed on the high binding energy side of the main core electron peaks. These satellite lines reflect the reorganization of the valence electrons upon core electron ionization, and are prominent in spectra from aromatic ring systems because of the high degree of delocalization of the π electrons.

Table 5.2: Parameters for N1s curve fitting of standard compounds

Compounds	**Alkyl chain length**	**Peak position (eV)**	**Full width at half maximum (eV)**	**Line shape**
poly(2-vinylpyridine)	0	398.8	1.0109	GL(35)
1-methylpyridinium iodide	1	401.2	0.8592	GL(35)
1-propylpyridinium bromide	3	401.3	0.9674	GL(35)
1-hexylpyridinium bromide	6	401.7	0.9566	GL(35)
1-hexadecylpyridinium bromide	16	401.8	0.9493	GL(35)

The XPS spectra of the standard compounds in this study are in good agreement with available data obtained from model compounds (Table 5.1). We used the parameters in Table 1 to fit N6 and NQ fractions. The peak position for N5 and nitro-type nitrogen is 400.2 ± 0.2 eV and 405.8 ± 0.2 eV, respectively (Biniak et al., 1997).

It should be noted that fitting an XPS spectrum cannot be rigorously accurate. Even if the number of unknown parameters is restricted as much as possible, the final accuracy remains limited. To assist with the precise identification of chemical groups, a chemical reaction specific to only the functional group of interest can be performed (chemical derivatization). For the work herein, methyl iodide has been used as a quaternizing reagent reacting with pyridine (N6) to form methyl pyridinium (NQ). The literature indicates that pyrroles (N5) do not react with methyl iodide under these conditions. In addition to the nitrogen characterization described above (increase of NQ fraction or decrease of N6 fraction), the degree of pyridine derivatization may then be measured by quantifying the iodine (3d5/2) peak at 617.9 eV.

5.1.2 Hi-resolution XPS spectrum for carbon 1s and oxygen 1s

Different peaks were used to curve-fit the XPS carbon 1s spectrum: aromatic and aliphatic groups (at 284.8 eV); C−O or C−N single bond (e.g. phenolic, alcohol, ether, or amine groups, at 285.6±0.2 eV); O=C or C=N double bonds (e.g. carbonyl or quinone groups, at 287.5 ± 0.2 eV), and carboxyl or ester groups (at 288.9 ± 0.2 eV). Carbonate, absorbed carbon dioxides, or the satellite peak due to $\pi - \pi^*$ transitions in aromatic systems are likely responsible for the binding energy of 290 ± 0.2 eV (Biniak et al., 1997; de la Puente et al., 1997; Moreno-Castilla et al., 2000). When the carbonaceous materials were submitted to treatments which modify either their structure and/or their chemical composition, not only the chemical shift of carbon 1s peaks, but also the C−C part are affected through incorporation or elimination of foreign elements (like N or O). An asymmetric line-shape was used to curve-fit the graphitic peak (Estrade-Szwarckopf, 2004).

Table 5.3: Literature assignments of the BE of the most common oxygen species present in carbon materials

Type of O	(1)[1]	(2)[2]	(3)[3]	(4)[4]	(5)[5]	material	ref
	531.1	534.2	533.3		535.9	Activated carbons	(Figueiredo et al., 1999)
	531.1	532.3	533.3	534.2	536.1	Carbon fibers	(Zielke et al., 1996)
	531	533			535	Activated carbons	(de la Puente et al., 1997)
BV (ev)	531.4	533		534.4		Coal	(Grzybek & Kreiner, 1997)
	531.5	533.5	533	532.3	535.5	Carbon fibers	(Kozlowski & Sherwood, 1985)
	531.4	533.7	532.4		535	Carbon nanofiber	(Arrigo et al., 2010)
	531.6	532.4		533.6	535-6	Carbon fibers	(Desimoni et al., 1992)

[1−4] Oxygen functional groups as shown in Figure 5.2

[5] Adsorbed H_2O

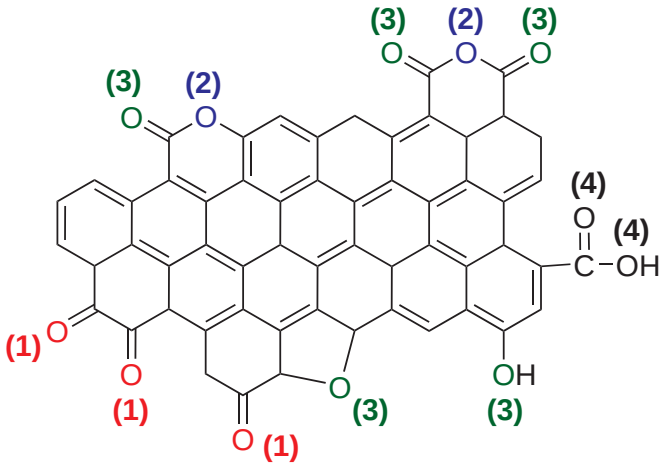

Figure 5.2: Oxygen functional groups determined by XPS at their corresponding binding energies given in Table 5.3. (adapted from Zielke et al. (1996))

Table 5.2 also shows the BE values of the most common oxygen functionalities in carbon materials reported in the literature. However, no common interpretation of curve fitting of O1s yet exists. According to our analysis, the O1s XP spectrum can be divided into the following regions (Figure 5.2): O1 (531.1-531.5 eV) corresponds to highly conjugated forms of carbonyl oxygen such as quinine; O2 (532.3 eV) is the ether oxygen atoms in esters and anhydrides; O3 (533.3 eV) is assigned to carbonyl oxygen atoms in esters, amides, anhydrides and oxygen atoms in hydroxyls or ethers; O4 (534.2 eV) refers to the oxygen atoms in carboxyl groups; and O5 (535.5-536 eV) refers to adsorbed water and/or oxygen. It should be noted that the assignments of O1s are not entirely unambiguous.

5.2 Oxidation by nitric acid

5.2.1 Study on AC1240C carbon

Among common oxidizing methods (including H_2O_2, $(NH_4)_2S_2O_8$, O_3 and HNO_3) used to treat carbon materials, HNO_3 typically resulted in the highest levels of oxidation (Wepasnick et al., 2011). In this study, we varied the oxidation temperature (from 20 to 105 °C) to control the extent of oxidation. The nitric acid treatment resulted in a distinct decrease in the atom percentage of aromatic and aliphatic carbon (Table 5.4) as well as the increase of oxygen, and a slight percent increase of nitrogen (as oxidized nitrogen).

Table 5.4: Surface elemental composition (atom %, using XPS) for AC1240C carbon samples after nitric acid treatment in different temperatures

Oxidation temperature (°C)	**Carbon**	**Oxygen**	**Nitrogen**
Virgin	93.64	6.36	N.D.[1]
20	87.38	11.65	0.97
50	87.12	11.97	0.91
80	82.27	16.75	0.98
95	81.09	17.68	1.22
105	75.97	22.75	1.28

[1] Not detected

Using XPS analysis, the increase in oxidation as the temperature increased was clearly observed by comparing changes in the intensity of the O1s spectrum (Figure 5.3). The inserts in Figure 5.3 also show that various oxide surface functional groups are present in all the activated carbons. The C1s signal shows an asymmetric tailing, partially due to the intrinsic asymmetry of the graphitic peak and to the contribution of oxygen surface functionalities. Therefore, oxygen functional groups were introduced into the carbon surface, which were essential for creating reactive sites for subsequent tailoring.

The relative peak area percentage of different oxygen groups under different oxidation temperatures was calculated and ascribed to the fraction of surface functional groups (Figure 5.4). The atomic oxygen concentration increases linearly with increasing oxidation temperature. It can be seen that the nitric acid treatment increased all single- and double-bonded oxygen-containing groups and carboxylic groups. Although the level of oxidation can be controlled by varying the oxidation temperature, the distribution of surface oxygen functional groups is relatively independent of the reaction conditions. In a related study, Wepasnick et al. (2011) found that using chemical derivatization to analyze hydroxyl, carbonyl and carboxylic acid groups on commercially available multi-

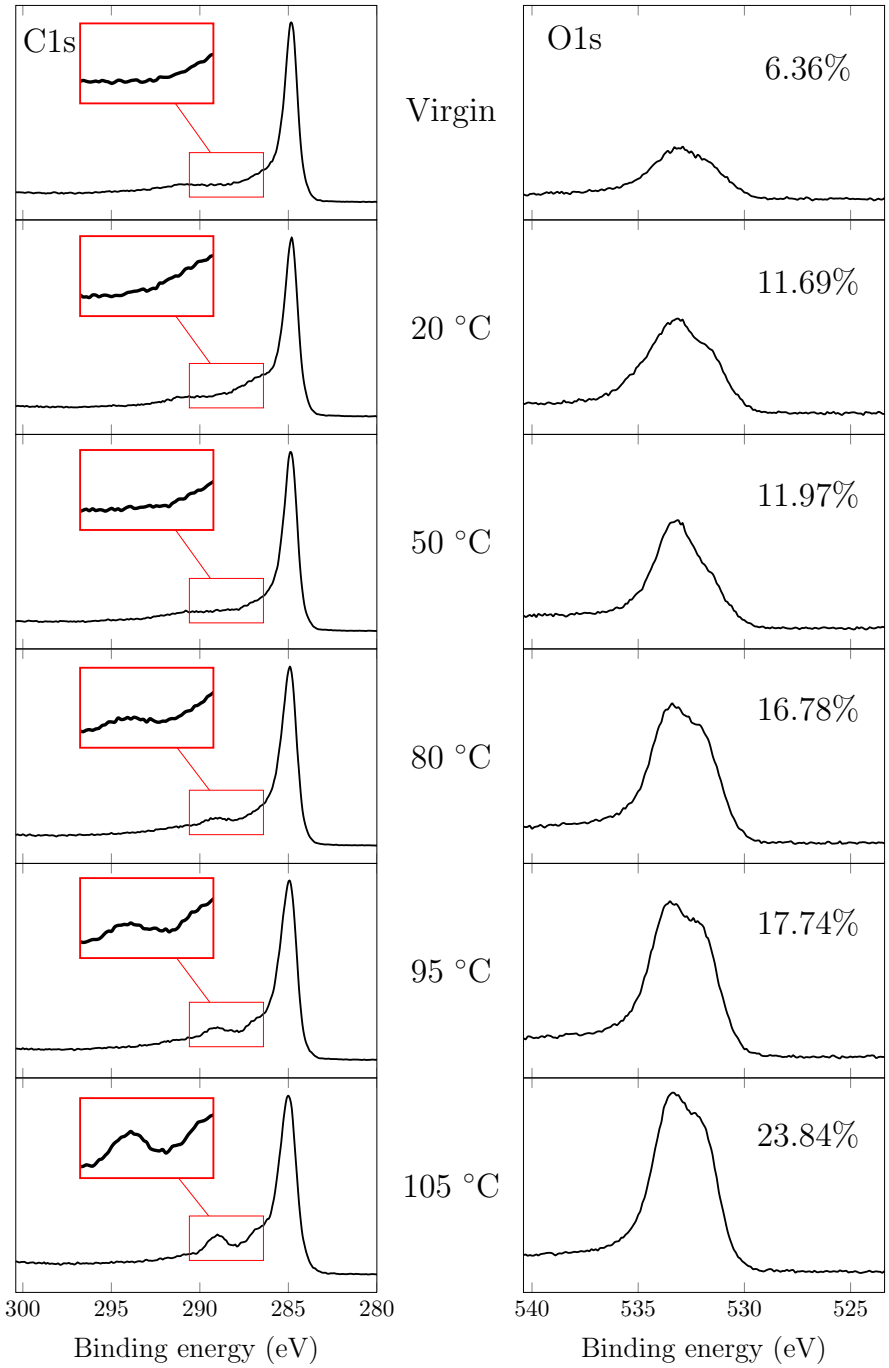

Figure 5.3: C1s and O1s XPS regions of AC1240C carbon oxidized by varying oxidation temperature of HNO_3.

walled carbon nanotubes (MWCNTs) that had been oxidized with different w/w% HNO_3 (from 0-70%), the concentration of all three functional groups increased compared to the untreated MWCNTs. In contrast to our results, Wepasnick et al. (2011) found that carboxylic acid groups (COOH) was the dominant species (roughly 50%); however, in our study the highest percentage of carboxylic acid groups is only 20% (at 20 °C). In our

study, the range of oxidation temperatures (20-105 °C) was much lower than the temperatures in the work of Wepasnick et al. (140 °C), which would effect the functional group distribution.

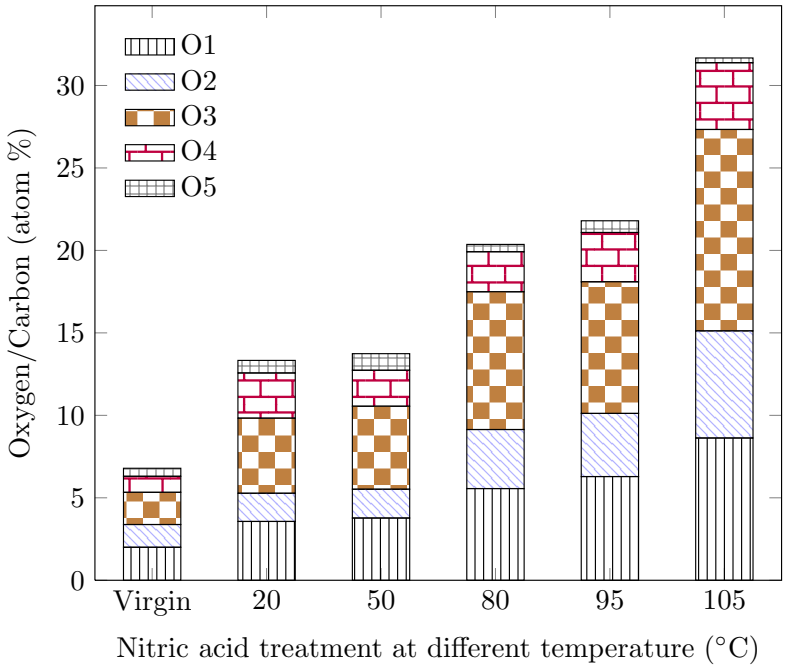

Figure 5.4: Surface atomic concentrations of different oxygen-containing groups as a function of nitric acid treatment temperature (AC1240C carbon)

Detailed analysis of the full width at half-maximum (fwhm) of the C 1s peak at 284.8 eV (graphite-like carbon) showed that activated carbon samples treated in nitric acid at higher temperature exhibited wider C 1s peaks than those treated at lower temperature (Figure 5.5). The fwhm of the graphite peak is related to the heterogeneity of the graphite layers. The nitric acid treatment destroyed the sp2 atomic structure of the polyaromatic sheets and resulted in wider graphite peaks (Li et al., 2009).

Several trends were observed when characterizing the acid treatment of virgin AC1240C carbon as shown in Figure 5.7. First, single-point adsorption volume consistently decreased with increasing oxidation temperature (Figure 5.7 a). Also, at the reflux temperature of nitric acid (105 °C), a drastic decrease in pore volume was observed. The loss of micropore volume was assumed to be related to the fixation of oxygen groups at the entrance and on the walls of micropores. Since pore volume values are reported as normalized to grams of activated carbon, an increase in weight from the oxidation process will result in lower pore volume values per unit weight. Moreover, the oxidation process also produced some by-products in the form of humic substances which could get lodged in the micropores resulting in loss of microporosity (Chingombe et al., 2005).

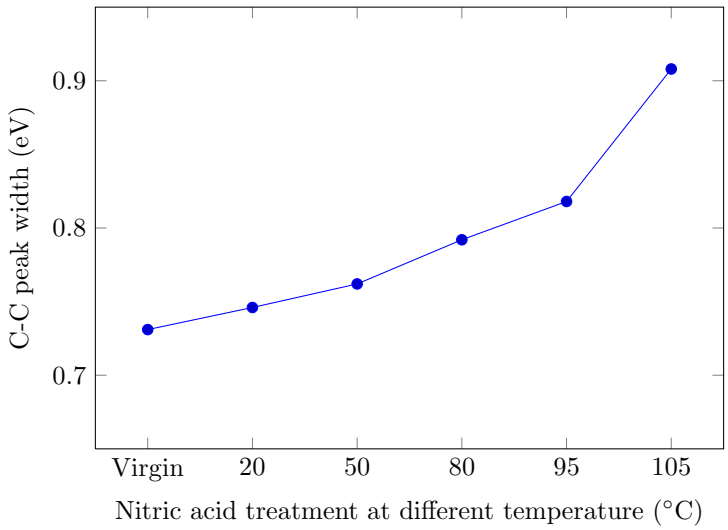

Figure 5.5: C-C 1s peak widths of AC1240C carbon samples after nitric acid treatment in different temperatures

Second, with increasing treatment temperature, the slurry pH consistently decreased (Figure 5.7 b). Slurry pH can be treated as an approximate measure of the pH at the point of zero charge (pH_{PZC}). According to a study by Chen et al. (2005a) the difference between the slurry pH and the pH_{PZC} is less than 2% for most of the carbons that are treated by acids or ammonia. Recall our results showed that the percentage of surface oxygen consistently increased with increasing temperature. It is known that stronger acidic functional groups are deprotonated at a lower pH while weaker acidic functional groups are deprotonated at a higher pH. Hence, these results implies that the nitric acid treatment increase the number of strong and weak acidic functional groups.

Methylene blue dye adsorption was employed as an alternative method for the determination of acidic surface functionality (Figure 5.7 c). This dye was previously used for characterization of activated carbon and carbon fibers (Pittman et al., 1997). Methylene blue adsorbs on carbon surfaces via a $\pi - \pi$ dispersion interaction as well as negatively charged sites. Krupa & Cannon (1996) found methylene blue adsorption to be strongly correlated with pore size smaller than 27 Å, which contains both micropores and mesopores. Here, methylene blue adsorption remained stable initially with increased oxidation temperature (up to 50 °C), then increased dramatically at higher temperature range (50-105 °C). It would appear that a combination of oxygen functionality, charge effects and pore size selection are controlling the adsorption of the lower treatment temperature carbons; conversely, carbon samples oxidized at 95 and 105 °C exhibit adsorption attributed to charge interaction between the negatively charged oxygen functional groups and the positively charged dye.

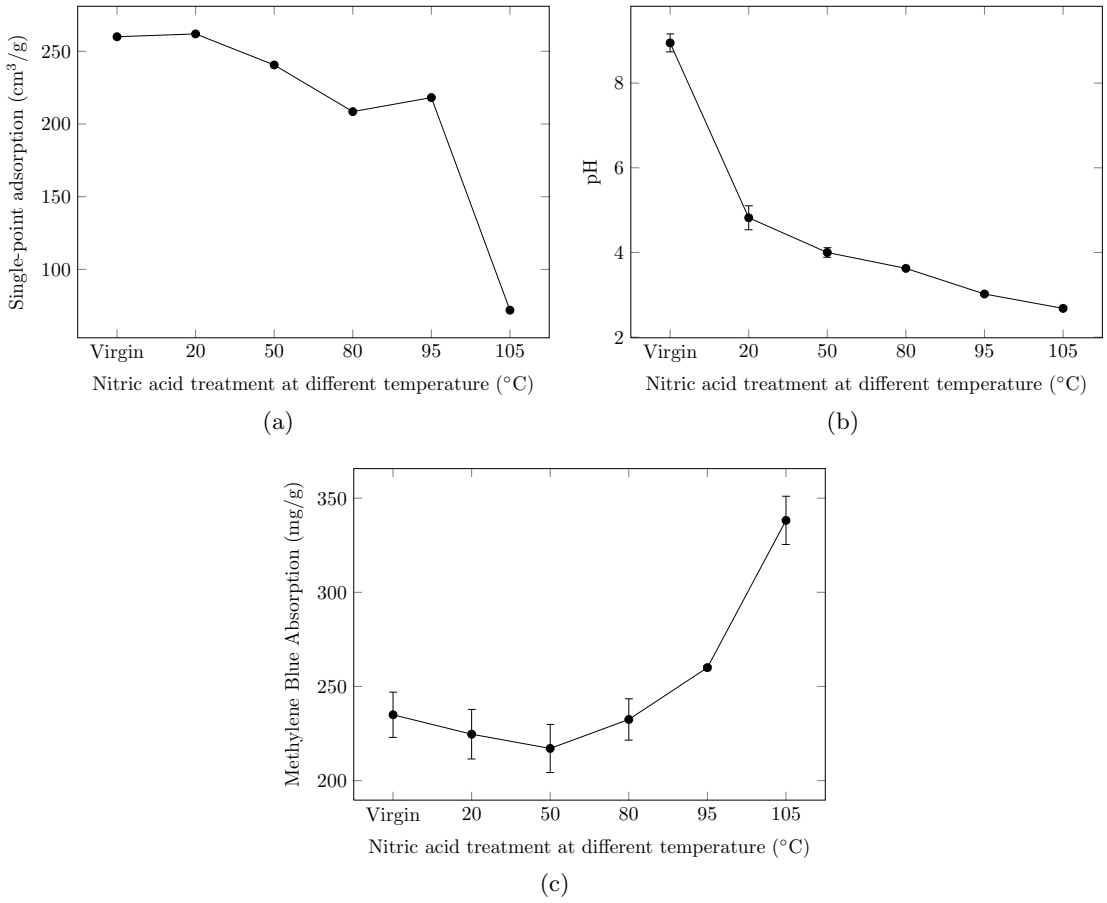

Figure 5.6: Effect of nitric acid treatment on single-point argon adsorption at 9.5×10^{-3} atm (a), slurry pH (b), and methylene blue dye adsorption (c) for AC1240C carbon samples (Data from Tim Byrne and Colin Cash)

5.2.2 Different activated carbon substrates

Besides AC1240C carbon, several other commercial available carbons were also investigated. UC1240 carbon shows similar trends as AC1240C carbon: as oxidation temperature increased, both pore volume and slurry pH gradually decreased (Figure 5.7). UC1240 carbon is a bit more "rigid" than AC1240C carbon, since treated at same temperature the drop of pore volume is less than the latter and the gain of surface oxygen is greater (Table 5.5).

AU and UC1240 carbons are relatively hard carbons with high apparent density which makes them somewhat resilient to acid treatments. The porosities of GC carbon was more affected by the acid oxidation treatments due to their low apparent densities and "softer" structure. Nitric acid treatment of GC carbon at 80 °C destroyed nearly all of the porosity (Figure 5.8), comparing to AC1240C carbon and UC1240 carbon oxidized at the same temperature the losses of pore volume (based on single-point adsorption)

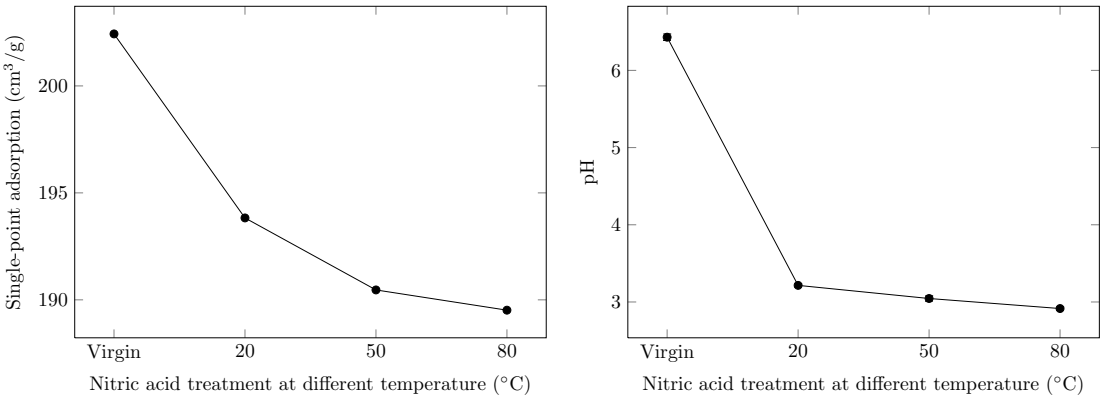

Figure 5.7: Effect of nitric acid treatment on single-point argon adsorption at 9.5×10^{-3} atm (a), slurry pH (b) for UC1240 carbon samples (Data from Tim Byrne and Colin Cash)

Table 5.5: Surface elemental analysis of virgin and nitric acid treated carbons (samples marked by designation plus the temperature of nitric acid treatment)

Sample	**O (%)**	**N (%)**	**C (%)**
UC1240	6.39	0.35	93.27
UC1240-50	10.32	1.17	88.51
UC1240-80	13.36	1.43	85.20
GC	10.4	0.53	88.79
GC-20	16.74	2.88	80.38
GC-80	24.84	2.88	72.28
RGC	4.22	N.D.[1]	95.78
RGC-20	8.94	1.25	89.82

[1] Not detected

are 19.81% and 6.38%, respectively, and it did introduce 24.8% oxygen by XPS analysis (Table 5.5). Oxidation of GC carbon at 20 °C decreased the total pore volume by about 25%, yet 16.7% oxygen resulted. Likewise, oxidation of RGC at 20 °C did not greatly reduce the total pore volume and results in 8.94% oxygen. GC and RGC carbons were produced by chemical activation using the phosphoric acid process. An increase in the degree of activation makes the pore walls thinner and, thus, more easily destroyed by the nitric acid oxidation (Moreno-Castilla et al., 1995).

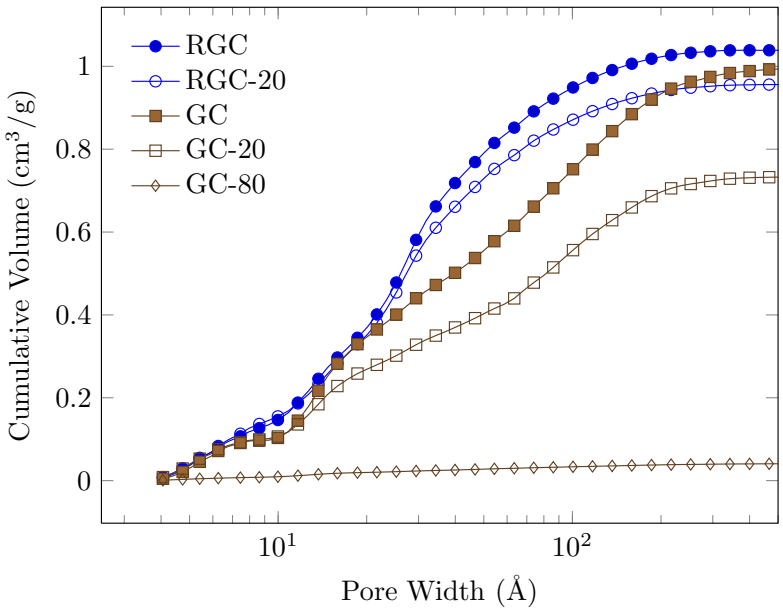

Figure 5.8: Cumulative pore volume distribution of virgin and nitric acid treated carbons, samples marked by designation plus the temperature of nitric acid treatment (Data from Tim Byrne)

5.3 Thermal treatment by ammonia

5.3.1 Influence of pre-oxidation

Table 5.6 shows the elemental composition of the ammonia treated AC1240C carbon samples. The thermal treatment in ammonia resulted in a significant decrease in the content of oxygen as a result of the decomposition of surface functional groups and a great increase of nitrogen content. The elemental surface composition obtained from the XPS analysis are also given in Table 5.6 for comparison with the bulk composition obtained by the elemental analysis. XPS cannot detect the content of hydrogen in carbon samples. Therefore, for the purpose of Table 5.6 the surface content of C + O + N sums to 100%. In contrast, bulk analysis contains other elements (e.g. S, P, Cl) and ash. As a result, the bulk contents of both carbon and nitrogen are lower than the surface contents. However, the divergence between bulk contents and surface contents increased with nitrogen contents, indicating that the polyaromatic sheets closer to the surface were the one contained more nitrogen.

The differences in nitrogen and oxygen contents between the pre-oxidized and ammonia treated samples indicated that the presence of oxygen functionalities on the carbon surface before ammonia treatment played an important role in determining the degree of nitrogen incorporation to the surface, and pre-oxidation of carbons considerably en-

Table 5.6: Surface and bulk elemental analysis of ammonia treated (at 700 °C) AC1240C carbon (samples marked by designation plus the pre-oxidation temperature), obtained with XPS spectra (i.e. surface) and C and N elemental analysis (i.e. bulk)

		Nitrogen		Carbon	
Sample	**Oxygen**	surface	bulk	surface	bulk
AC1240C-N	2.59	2.18	2.04	95.23	93.19
AC1240C-O-20-N	3.31	2.46	2.28	94.23	92.78
AC1240C-O-50-N	3.45	3.63	3.21	92.92	92.11
AC1240C-O-80-N	2.89	5.95	4.88	91.16	89.55
AC1240C-O-95-N	2.2	6.09	4.91	91.7	89.59
AC1240C-O-105-N	3.56	7.2	5.88	89.24	87.85

hanced the nitrogen incorporation during the ammonia treatment (Figure 5.9). The process of oxidation enhanced the nitrogen introduction into the polyaromatic sheets by the reaction with ammonia at high temperature, as the nitrogen functional groups are bonded via oxygen-containing groups introduced earlier.

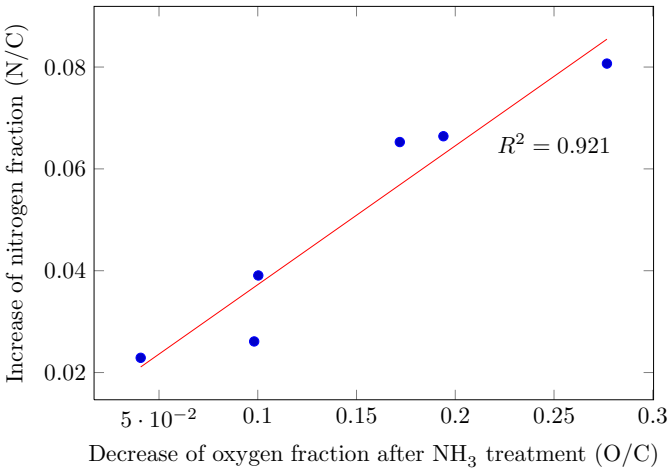

Figure 5.9: Relationship between the extent of pre-oxidation on nitrogen tailoring

The curve fitting results on N1s high resolution spectrum of ammonia treated AC1240C carbon under different pre-oxidation conditions were shown in Figure 5.10. The distribution of nitrogen species remained constant regardless of the level of pre-oxidation. As discussed above, the relative percentage of oxygen species on carbon surface oxidized at different temperature is invariant, suggesting that nitrogen is introduced into the polyaromatic sheets through oxygen-containing groups.

The fwhm values for the C1s peak are plotted against the respective nitrogen doping levels in Figure 5.11. The fwhm values for ammonia treated carbon samples increase with additional nitrogen content, while the fwhm values are notably lower than these after oxidation. Broadening of the peaks in C1s spectra have also been attributed to

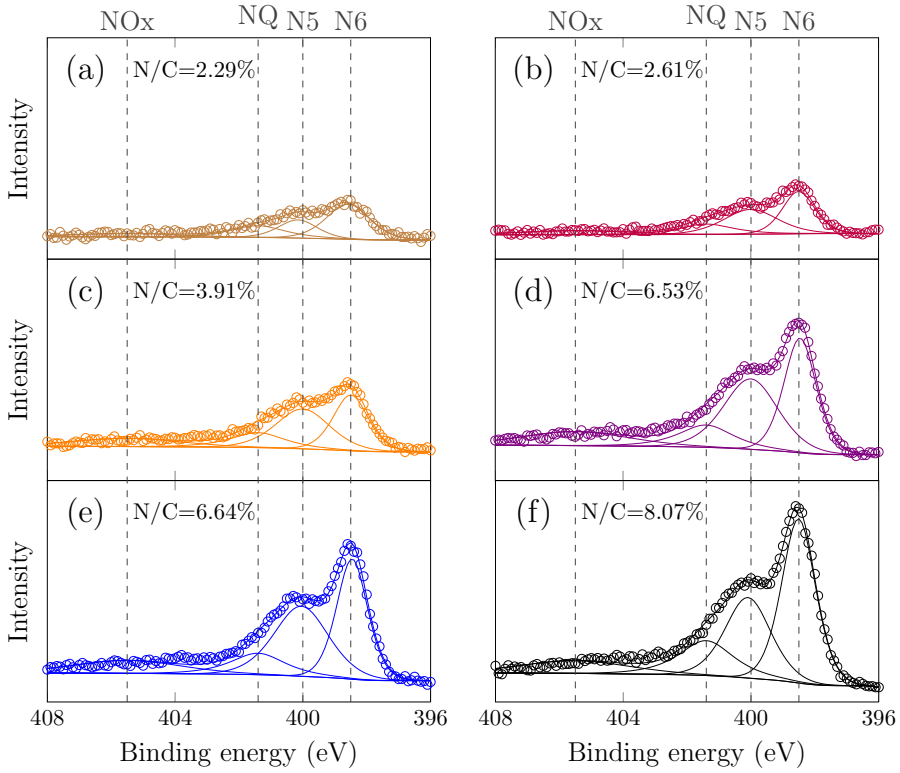

Figure 5.10: High-resolution N1s spectra for ammonia treated AC1240C carbon: (a) non-oxidized (virgin), preoxidized at (b) 20 °C, (c) 50 °C, (d) 80 °C, (e) 95 °C, and (f) 105 °C with N6 (pyridinic N), N5 (pyrrolic N), NQ (quaternary N), and NOx (nitro N).

lattice disorder in polyaromatic sheets.

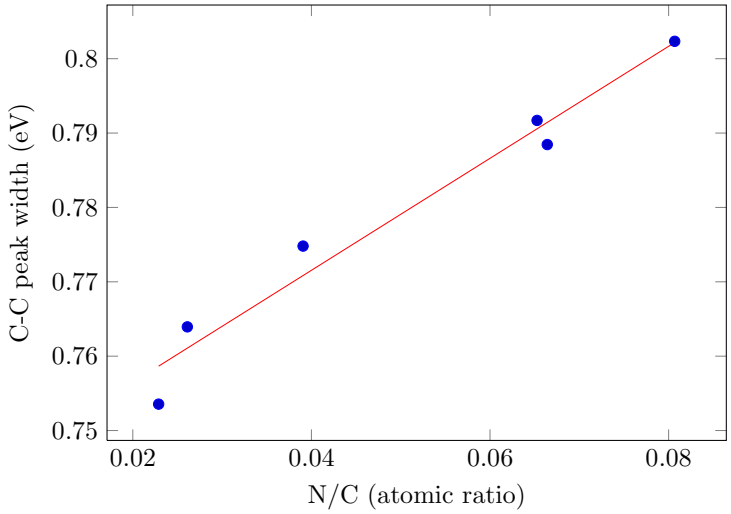

Figure 5.11: Full width at half maximum (fwhm) of the C1s spectra as a function of nitrogen content.

5.3.2 Influence of ammonia fraction

The ammonia fraction is another factor that affects the nitrogen tailoring process. Increasing the ammonia fraction in the carrier gas stream yielded a positive increase in the nitrogen doping process (Figure 5.12). Figure 5.12 also shows the sensitivity of the total nitrogen content with varying fractional amount of ammonia at a constant temperature (700 °C). It is very interesting that as low as 5% ammonia in the carrier gas was able to achieve a nitrogen content of 6.7 % and the ammonia fraction above 20% showed no additional influence on increasing nitrogen content. The N1s curve fitting results of carbon sample in different ammonia flow rate were similar.

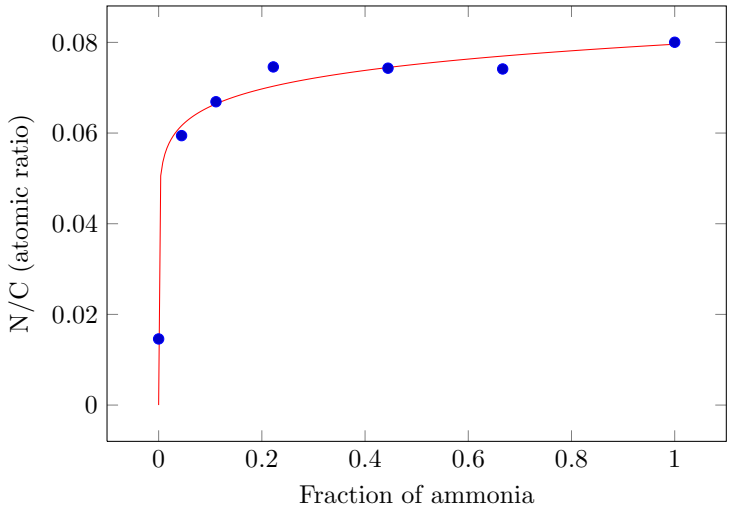

Figure 5.12: Relationship between fraction of ammonia and nitrogen content on carbon surface during amination of AC1240C carbon (pre-oxidized at 105 °C)

Figure 5.13 shows pore volume distribution of ammonia treated samples with different ammonia fractions. The decomposition of oxygen functional groups likely leads to some pore widening even in an inert atmosphere. However, it is clear that amination process notably increases both micro and meso pores. Maldonado et al. (2006) demonstrated that decomposition of ammonia in the presence of carbon-containing materials generates free radical species, e.g., $NH_2\cdot$, which may attack graphitic carbon and hasten its gasification to methane and cyanogen species.

5.3.3 Influence of amination temperature

The surface functional groups generated on the carbon surface through ammonia treatment at different temperatures were analyzed by XPS in both survey and high-resolution mode. Figure 5.14 shows the XPS survey spectra of the AC1240C carbon samples treated

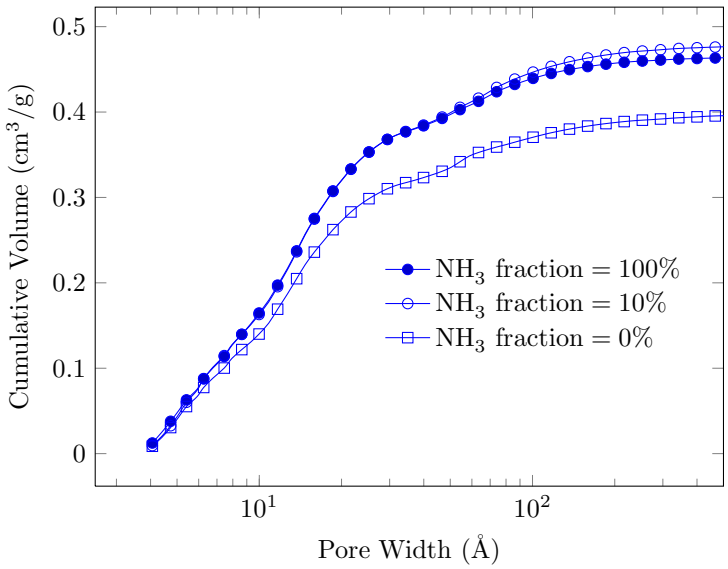

Figure 5.13: Cumulative pore volume of ammonia treated samples (UC1240 carbon pre-oxidized at 80 °C) with different ammonia fractions (Data from Tim Byrne)

in ammonia in comparison to pre-oxidized samples. All the spectra show a strong C1s peak at 284.8 eV of graphitic carbon. The AC1240C carbon oxidized with nitric acid have a significantly stronger O1s peak at about 532 eV, as well as a tiny N1s pick at about 405 eV, indicating the existence of nitro species. However, after exposing the pre-oxidized sample to ammonia at 450 °C, a strong N1s peak at about 400 eV appears, and the O1s peak intensity decreased almost by a factor of 3. With increasing amination temperature, the intensity of both the N1s and O1s peaks decreased gradually.

The surface atomic concentrations of C, O, and N were derived from the corresponding peak areas of the XPS spectra and are summarized in Table 5.7. Treatment of AC1240C carbon with nitric acid at 105 °C generates a large amount of oxygen with a surface atomic concentration as high as 19.4% on the carbon surface. The treatment at 450 °C created a maximum amount of nitrogen species (8.91%). After the treatment of the pre-oxidized carbon samples in ammonia at 800 °C, only 5.94% of nitrogen and 5.28% of oxygen were present on the carbon surface.

Figure 5.15 shows the curve-fitting results of XPS N1s high-resolution spectra of the carbon samples obtained by treatment of the pre-oxidized AC1240C carbon in ammonia at 450, 600, 700 and 800 °C. As treatment temperature increased, different overall N1s peak line shapes were observed reflecting a different distribution of nitrogen species.

To highlight the change in the distribution of nitrogen species with increasing temperature of functionalization, the abundance of all nitrogen components is shown in Table 5.7 and Figure 5.16. It is clear that NOx type nitrogen (pyridine-N-oxide or nitro) is the

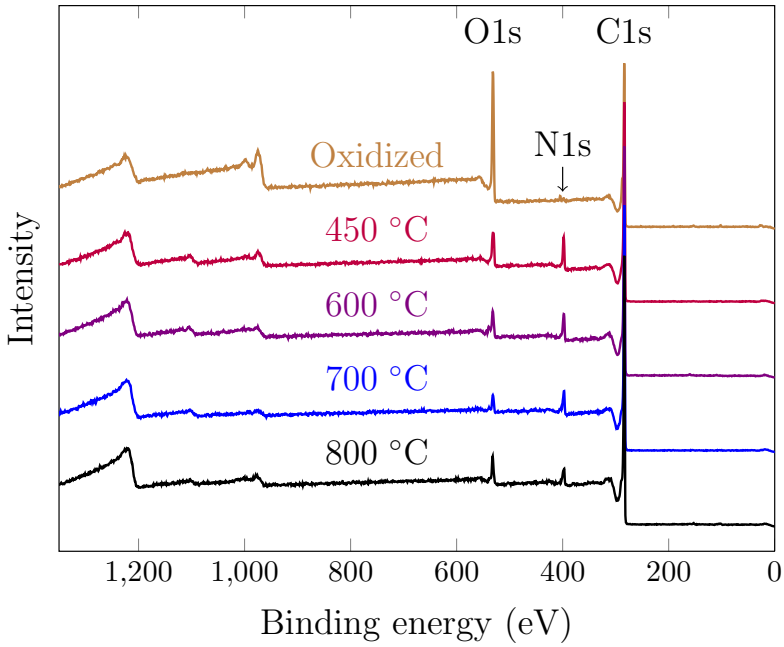

Figure 5.14: XPS survey spectra of AC1240C carbon treated in ammonia at various temperatures (shown above the line)

Table 5.7: Surface composition (using XPS) of oxidized AC1240C carbon (oxidized with nitric acid at 105 °C, designated as AC1240C-O) and ammonia treated carbon (samples marked by designation N plus the temperature of ammonia treatment)

			Nitrogen				
Sample	**Carbon**	**Oxygen**	**N-total**	**N6**	**N5**	**NQ**	**NOx**
AC1240C-O	75.97	22.75	1.28	0.09	0.05	0.31	0.83
AC1240C-N-450	82.9	8.19	8.91	2.96	4.22	0.83	0.90
AC1240C-N-600	83.84	8.82	7.34	2.85	2.89	0.88	0.72
AC1240C-N-700	89.24	3.56	7.2	3.08	2.25	1.09	0.77
AC1240C-N-800	88.78	5.28	5.94	2.81	0.81	1.87	0.45

most abundant species for the pre-oxidized carbon sample (65% of the total nitrogen). Treating the pre-oxidized carbon sample at 450 °C in ammonia increased the amount of N5 species reaching its maximum value of about 4.22% (47.4% of the total nitrogen). When further rising the treatment temperature to 600 °C, 700 °C and 800 °C, the N5 species decreased gradually to 2.89, 2.25 and 0.81%, respectively. In contrast, the NQ species shows a gradual increase with increasing treatment temperature in ammonia. For the sample treated at 800 °C, about 31.48% of the total nitrogen was quaternary-type nitrogen. The amount of N6 species remained relatively constant at different ammonia treatment temperatures, however the percentage of N6 species gradually increased as temperature increased.

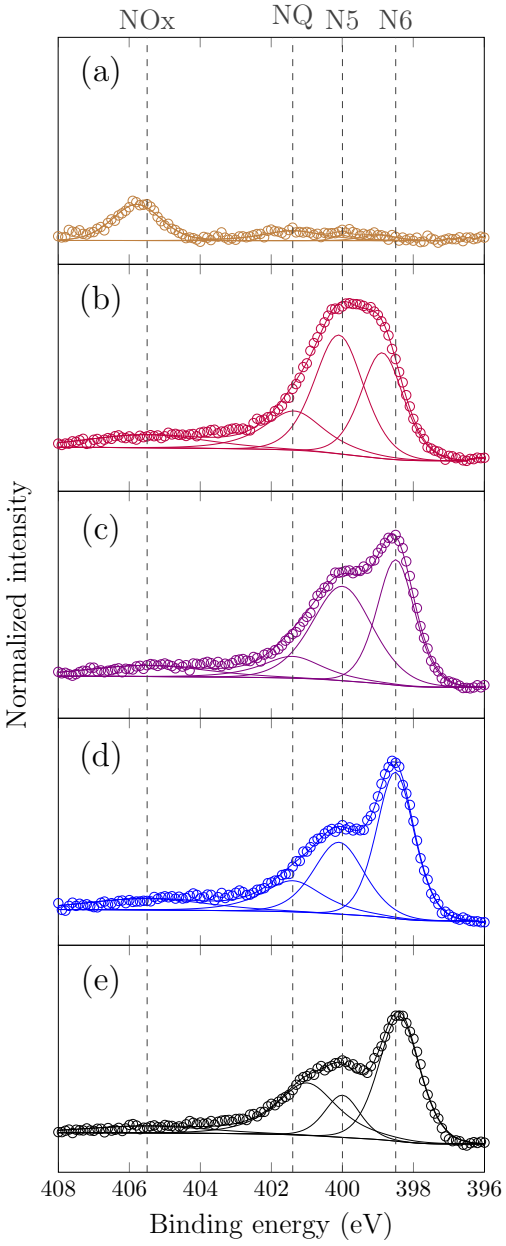

Figure 5.15: High-resolution N1s spectra for AC1240C carbon: (a) oxidized with nitric acid at 105 °C, obtained by ammonia treatment of pre-oxidized carbons at (b) 450 °C, (c) 600 °C, (d) 600 °C, and (e) 800 °C with N6 (pyridinic N), N5 (pyrrolic N), NQ (quaternary N), and NOx (nitro N).

In section 5.2, we have shown that the nitric acid treatment mainly creates carboxyls, lactones, hydroxyls (phenols), pyrones (ether-type), and carbonyls. The possible reactions of these functionalities with ammonia on the pre-oxidized carbon surfaces during heating in ammonia are depicted below:

- Carboxylic group: Ammonium salts are formed upon treatment of carboxylic acids

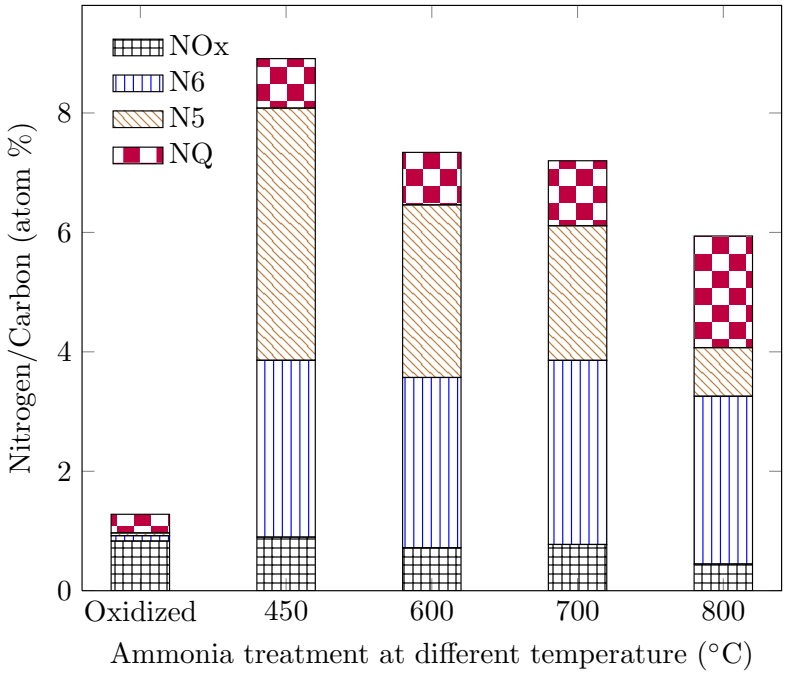

Figure 5.16: Surface atomic concentrations of different nitrogen-containing groups as a function of ammonia treatment temperature (AC1240C carbon)

in ammonia at room temperature, and they are thermally dehydrated to carboxylic amides at 80 °C and nitriles at 180-200 °C (Kundu et al., 2010).

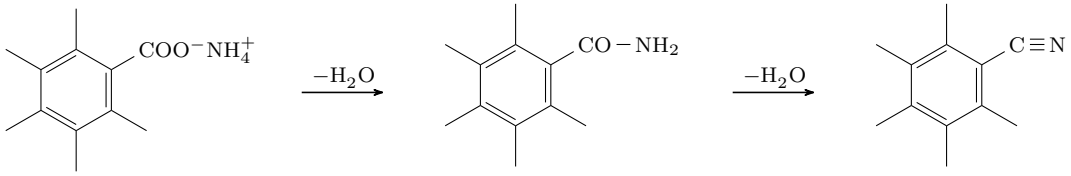

For carboxyl groups or adjacent carboxyl groups in the defective sites on graphitic surfaces, during the initial stages of heating, ammonia reacts with carboxylic acid to form intermediate, possibly amide, lactam, or imide species (Stohr et al., 1991; Jansen & van Bekkum, 1994). As the treatment temperature increasing, those species undergo dehydration or decarbonylation reactions to form more stable heterocyclic aromatic moieties (pyrrole or/and pyridine).

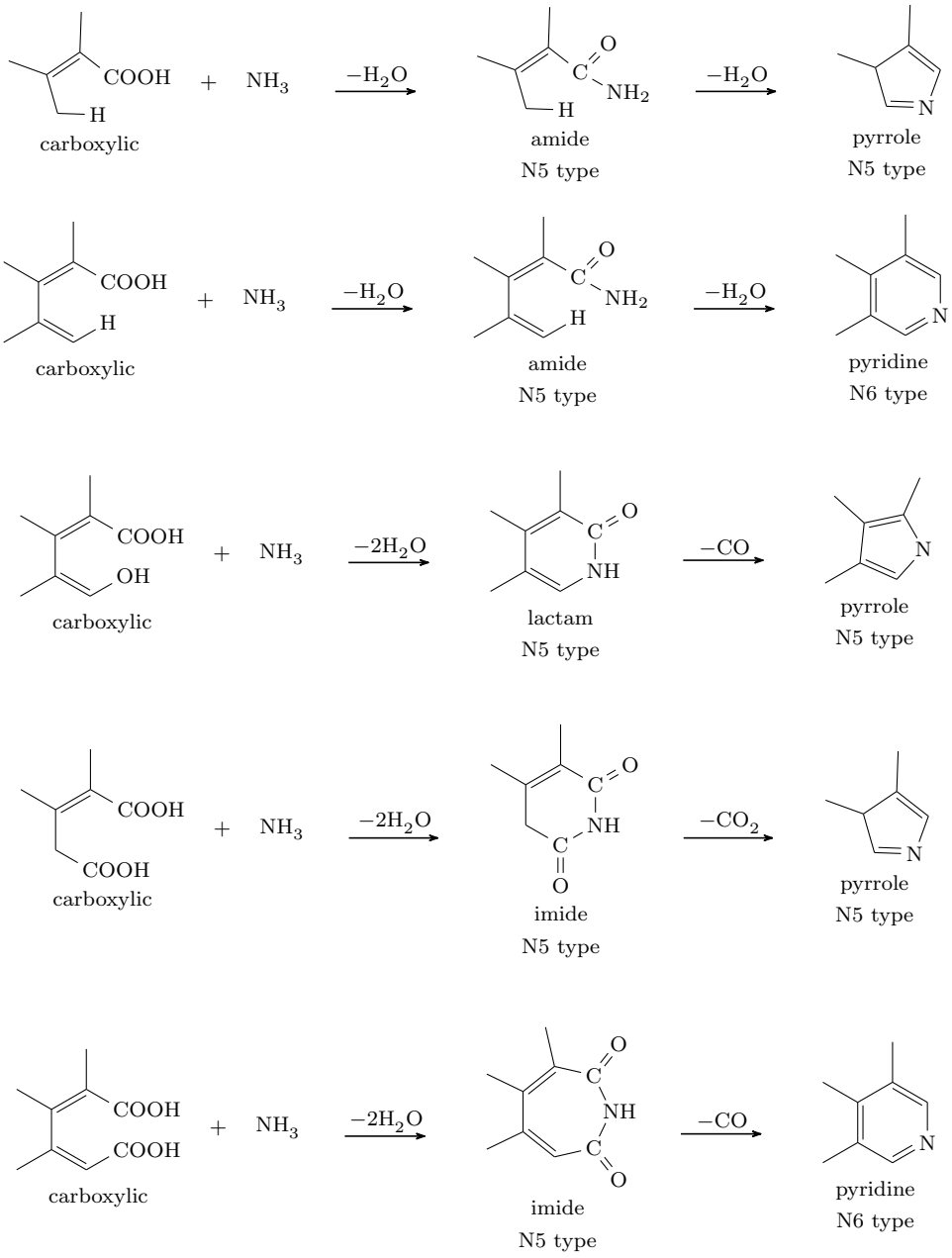

- Lactone: The reaction of ammonia with lactone groups can lead to the formation of lactams, which may lead to pyrrole groups by releasing CO at temperature higher than 450 °C (Kundu et al., 2010).

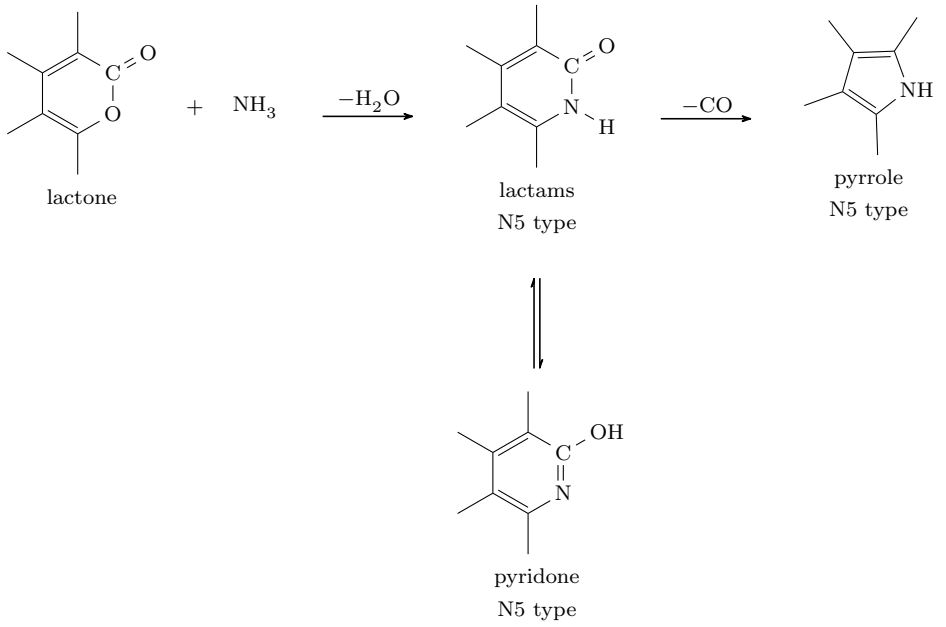

- Ether: The ether-type oxygen can readily react with ammonia via dehydration, and further dehydrogenation can lead to the formation of pyridine.

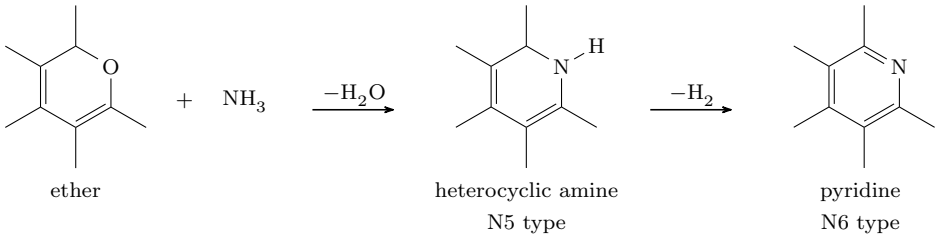

- Phenol: Kundu et al. (2010) claimed that amines can be formed via substitution of phenolic groups:

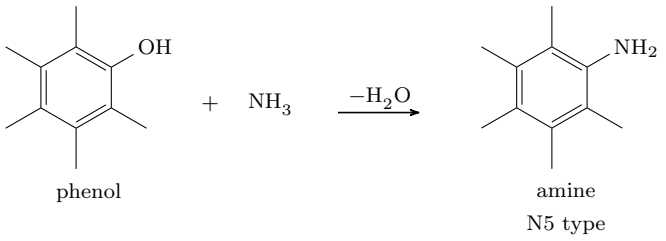

On the contrary, Li et al. (2009) found that ammonia could only be introduced on the surface of graphene oxide pre-reduced in H_2 below 500 °C. Below that temperature, phenol, quinone and alcohol would not start to decompose, implying these functional groups may not involve in the amination process. However, de la Puente et al. (1997) suggested that lactones or ether bridges between rings could be formed from phenol with neighbouring aromatic carboxylic acids or hydroxyl groups during heating treatment. Through this pathway, phenol (or alcohol) group might react with ammonia at high temperature.

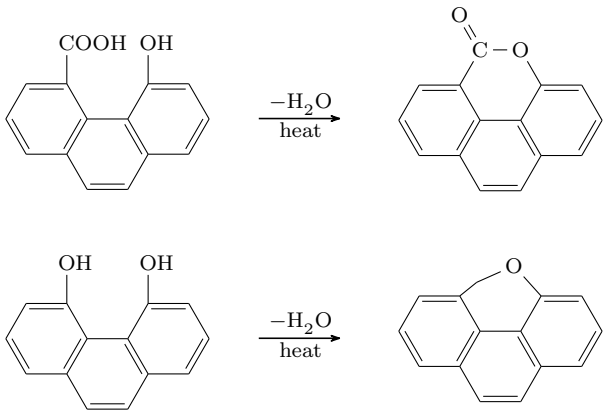

At low temperature, some intermediates such as amide, lactam and imide were formed. As the temperature increasing, these functional groups are preferentially converted to pyridinic and pyrrolic nitrogen species in the carbon structure during heat treatment. This is probably because the defect-containing polyaromatic sheets have sufficient energy to undergo rearrangement and remove the defects such that the most thermodynamically stable structure is formed (heterocyclic aromatic moieties). Our data suggested that higher ammonia treatment temperature afforded more quaternary nitrogen incorporated into the carbon network of polyaromatic sheets. On the other hand, increasing the functionalization temperature results in competitive nitrogen species as well as ammonia decomposition (Arrigo et al., 2010; Kundu et al., 2010). This is also a reason why it is more difficult to introduce larger amount of nitrogen species at higher temperature. Based on this data, the treatment temperature of 700 °C was used for majority of tested samples as it had the best pyridine-like fraction (N6).

5.4 Quaternization reaction

5.4.1 Qualitative analysis of pyridinium species

The goal of quaternization is to convert available edge site pyridine groups into pyridinium groups. The extent of this conversion was monitored by XPS by determining both the iodide or bromide fraction that remains on the carbon surface as counter ions to balance the charge of produced charged pyridinium groups or amount of N6 that converted to NQ after quaternization treatment.

After methyl iodide treatment, the total content of nitrogen remained constant. However, the functionality of nitrogen changed: part of the N6 fraction was converted to the NQ fraction, while the N5 fraction remained constant (Figure 5.17). Conversion of from N6 to NQ via analysis of the N1s spectrum from XPS was also confirmed by Perrier

& Benerito (1975) for quaternization of quaternary ammonium cellulose cottons using methyl iodide.

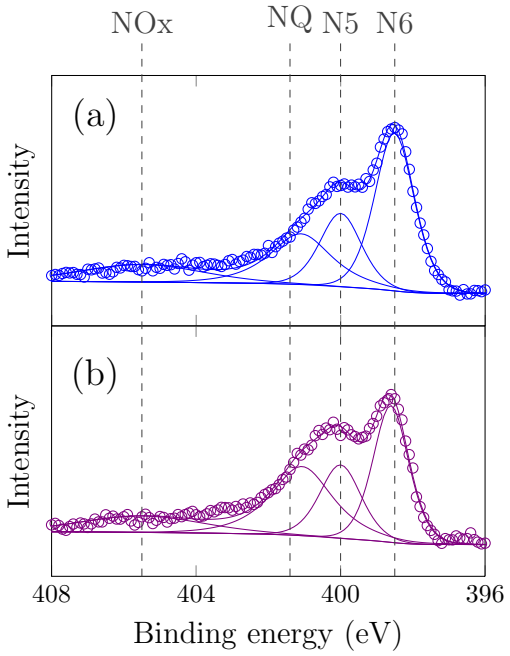

Figure 5.17: High-resolution N1s spectra for modified AC1240C carbon (pre-oxidized at 80 °C): (a) ammonia treated at 700 °C, and (b) methyl iodide treated after amination with N6 (pyridinic N), N5 (pyrrolic N), NQ (quaternary N), and NOx (nitro N).

Recall that methyl iodide is used as a quaternizing reagent according to the following equation:

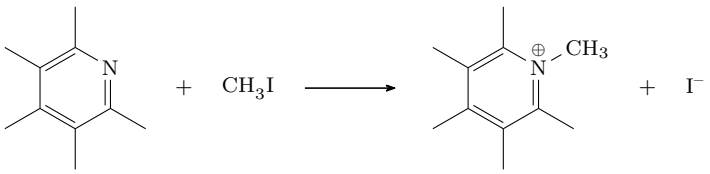

Pyrroles do not react with methyl iodide under these conditions. The degree of pyridine derivatization may then be measured by quantifying the iodine (3d5/2) peak at 617.9 eV. However, methyl iodide is an strong nucleophilic reagent for SN2 substitution reactions and can react with many oxygen or nitrogen containing functional groups (e.g. carboxylic acid, phenol, alcohol and amine). Moreover, methyl iodide as an organic compound with a high molecular weight may adsorb onto the surface of activated carbon. So a control sample was set up in which the typical thermal treatment was carried out except for in an inert nitrogen atmosphere instead of ammonia, then this sample was treated in methyl iodide as well. In this case, the iodine fraction in the control sample is treated as the background to determine the “active” pyridine (or pyridinium) fraction.

Figure 5.18 shows the relationship between iodine fraction and the change of NQ fraction for methyl iodide treated AC1240C carbon samples. The iodide fraction in Figure 5.18 is calculated as: $I_{fraction} = I_{measured} - I_{background}$. As indicated in Figure 5.18, the pyridinium fraction determined by the I fraction showed strong consistency with the value determined by increase of NQ fraction, as all the data were near the 45-degree line.

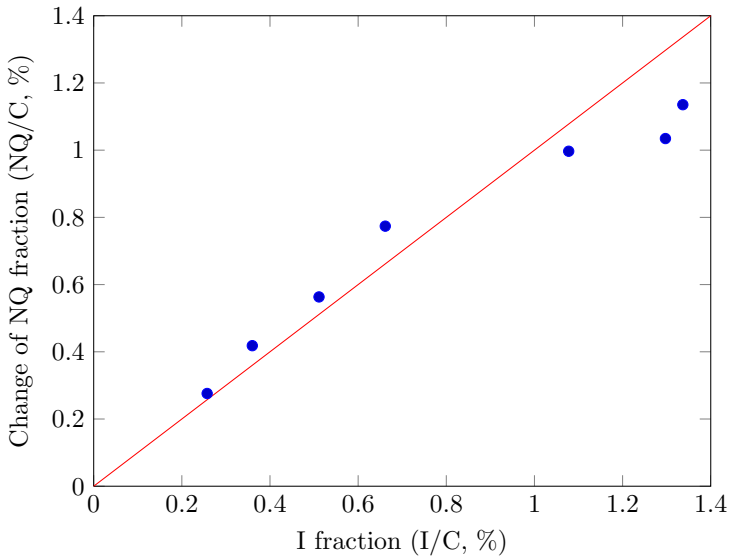

Figure 5.18: The relationship between iodine fraction and the change of NQ fraction, solid line is $y = x$.

As discussed above, the pre-oxidation greatly enhanced the total nitrogen content, though the distribution of nitrogen species remained constant. As a logical extension, the quaternized sample which is pre-oxidized at the highest temperature would have the highest pyridinium content. However, Figure 5.19 shows the sample pre-oxidized at 80 °C had the highest pyridinium content, in which the total nitrogen content is not the highest one. The pyridinium species is converted from accessible pyridine at the edge of the polyaromatic sheets. For the samples oxidized at temperature higher than 80 °C, the pore structure is partially destroyed, which make the pyridine site less accessible.

5.4.2 Effect on the pore structures

Table 5.8 lists the micropore, mesopore volume and specific surface area of virgin, nitric acid treated, ammonia treated and methyl iodide treated carbons while Figure 5.20 shows their cumulative pore volume distribution. The data in Table 5.8 demonstrate that nitric acid treatment of the activated carbons leads to an appreciable loss of the total surface area (from 4.8 to 18.4%) and a small increase in the mesopore volume with

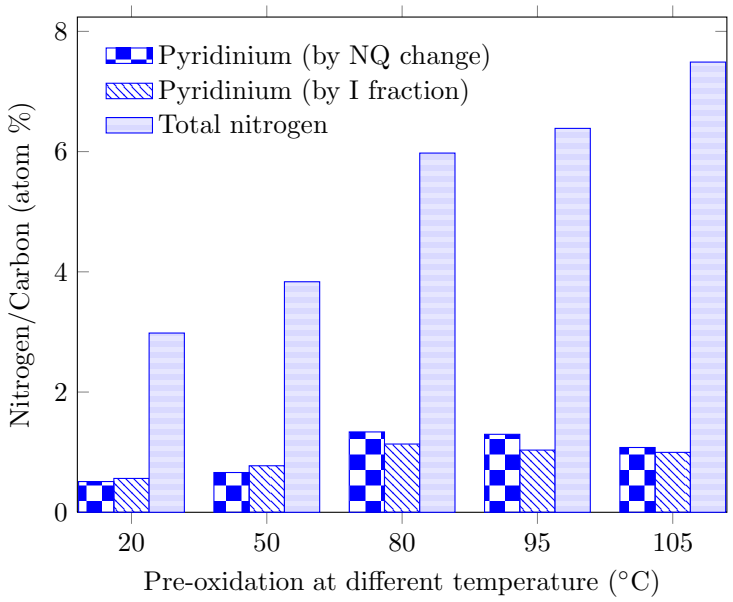

Figure 5.19: Effect of pre-oxidation on total nitrogen and pyridinium fraction (determined by I fraction and increase of NQ fraction) for quaternized AC1240C carbon samples

some widening of the average pore width, indicating effective attack by nitric acid by causing partial destruction of polyaromatic sheets.

Ammonia treatment enlarged the total pore volume (mainly mesopores) and the average pore width indicating that ammonia was acting as an etchant. Wang et al. (2010) also demonstrated that after ammonia treatment at high temperatures, both BET surface area and pore volume increased compared to the pristine carbon material. It has been surmised that the radicals ($NH_2\cdot$, NH· and atomic hydrogen) generated from ammonia decomposition at high temperature would cause some gasification of the carbon material; and it also could have caused degradation of non-carbon impurities (Chen et al., 2005a). On the contrary, the GC carbon exhibited an identical adverse effect of ammonia treatment, shown by a decrease in the total surface area accompanied by large changes in pore volumes in different size ranges (total, meso- and micropores) and average pore width.

After methyl iodide treatment, the surface area and the volumes of micropores and mesopores decreased considerably for all the carbon samples. Similarly, Shi et al. (2007) observed that both surface area and the pore volumes of activated carbon decreased after tailoring with quaternary ammonium groups.

Table 5.8: Parameters of porous structure calculated from argon adsorption/desorption isotherms for the modified carbon samples, O:nitric acid treatment, N:ammonia treatment, Q:methyl iodide treatment (Data from Tim Byrne)

Sample	**BET area (m^2/g)**	**Micropores (< 20 Å) volume (mL/g)**	**Mesopores (20-500 Å) volume (mL/g)**	**Pore width (Å)**
AC1240C	1077.32	0.399	0.022	0.782
AC1240C-O	878.62	0.369	0.056	0.968
AC1240C-N	857.72	0.363	0.116	1.117
AC1240C-Q	468.45	0.217	0.073	1.237
UC1240	852.23	0.313	0.115	1.004
UC1240-O	771.90	0.290	0.148	1.133
UC1240-N	786.18	0.307	0.158	1.183
UC1240-Q	707.39	0.286	0.127	1.170
RGC	1118.06	0.371	0.679	1.879
RGC-O	1064.05	0.353	0.607	1.805
RGC-N	1112.49	0.364	0.694	1.901
RGC-Q	982.12	0.324	0.612	1.905
GC	910.48	0.348	0.651	2.195
GC-N	826.08	0.273	0.479	1.820
GC-Q	437.24	0.148	0.349	2.274

5.5 Adsorption of perchlorate

5.5.1 Adsorption by virgin carbons

A wide variety of activated carbon sources with very different surface chemistries and pore volume distributions (Figure 5.9) were used to investigate the adsorption capacity for perchlorate. AC1240C carbon is a coconut-shell activated carbon with a very microporous structure. It had the best removal of perchlorate before tailoring. UC1240 carbon is a bituminous based carbon with an even distribution of pores across micropore and lower mesopore range. RGC carbon is a hardwood(oak)-based carbon which is phosphoric acid activated and then steam treated. It has a very open, mesoporous porosity and low apparent density. GC carbon is a softwood-based carbon, activated with phosphoric acid activation. This results in an open pore structure, but low slurry pH and high oxygen content.

The perchlorate breakthrough profiles in rapid small-scale column tests (RSSCTs) of four virgin (non-tailored) carbon samples have been presented in Figure 5.21. The bed volumes (BV) to initial breakthrough reached 1,400 for AC1240C carbon, which performed the best of all the tested carbons. On the contrary, there was no retention time for perchlorate with the GC carbon, which would be attributed to the negatively charged surface (highest oxygen content and lowest slurry pH). The UC1240 carbon (bituminous

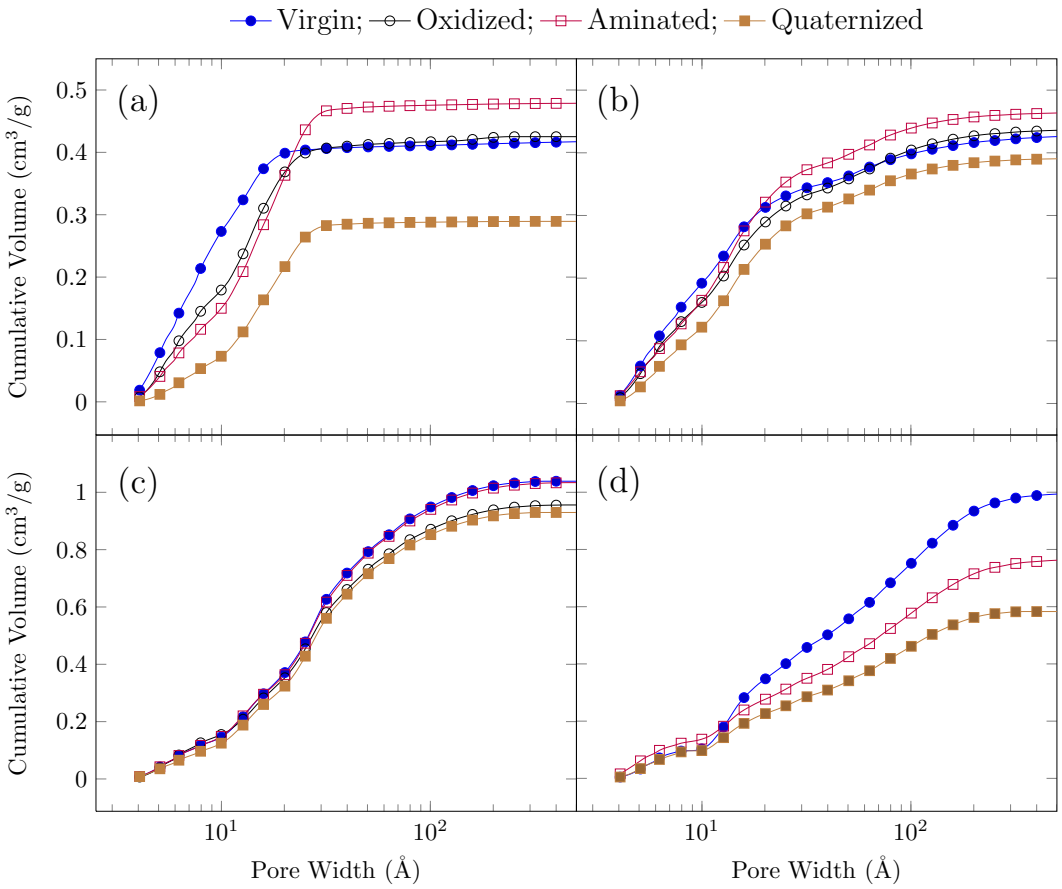

Figure 5.20: Cumulative pore volume distribution of modified carbon samples for (a) AC1240C, (b) UC1240, (c) RGC, and (d) GC carbons (Data from Tim Byrne)

Table 5.9: Physical chemical properties of the virgin carbon samples

Sample	**BET area (m^2/g)**	**Micropores volume (mL/g)**	**Mesopores volume (mL/g)**	**C (%)**	**O (%)**	**N (%)**	**Slurry PH**
AC1240C	859	0.399	0.022	92.23	7.770	N.D.[1]	8.95 ± 0.21
UC1240	967	0.313	0.115	94.71	5.290	N.D.[1]	6.43 ± 0.04
RGC	1460	0.371	0.679	95.78	4.220	N.D.[1]	9.00 ± 0.01
GC	1545	0.348	0.651	85.95	12.300	0.81	4.00 ± 0.02

[1] Not detected

coal based) had lower BET surface area and total pore volumes than GC and RGC carbons (wood based), but in fact had higher perchlorate adsorption capacity. This is in agreement with the data reported by Mahmudov & Huang (2010) who showed lignite and bituminous based activated carbons had expressed higher perchlorate adsorption than wood based activated carbons.

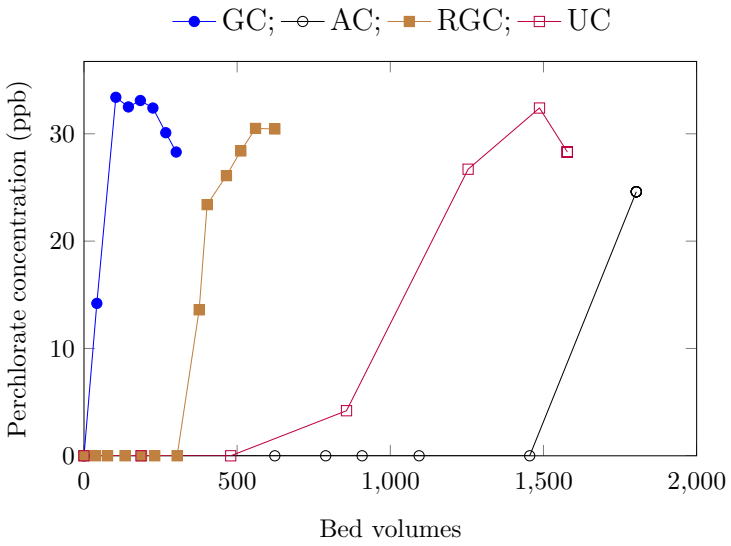

Figure 5.21: RSSCTs of perchlorate breakthrough by virgin carbons (Data from Tim Byrne and Pin hou)

5.5.2 Equilibrium adsorption of perchlorate

Adsorption isotherms of perchlorate onto both quaternized and non-tailored carbons are displayed in Figure 5.22. These tests employed deionized distilled water which was spiked with different concentration (30 ppb to 13.5 ppm) of perchlorate with 30 mg of carbon sample. Figure 5.22 indicates that quaternized carbons display significantly higher adsorption than virgin carbons, especially over low concentration range of perchlorate. It was observed that adsorption capacity reached an equilibrium value beyond which there was a negligible or no change in the residue perchlorate concentration (quaternized RGC carbon, Figure 5.22 d).

Four different alkylating agents were used to test the effects on perchlorate removal. Several different alkylation agents were used to compare the result of different length alkyl chains and different reactivities of the agents. CH_3I, C_3H_7Br, $C_6H_{13}Br$, and $C_{16}H_{33}Br$ were compared by perchlorate isotherms (Figure 5.22 a). However, methyl iodide was used the most because it was shown to be the most effective perchlorate removal though it was the most reactive (see Figure 5.22 a).

5.5.3 RSSCTs for perchlorate breakthrough

The increased adsorption capacities for perchlorate, created by the tailoring of pyridinium species are shown in Figure 5.23. For UC1240 carbon, initial detection of perchlorate in the RSSCTs effluent was observed at 900 BV, with full breakthrough of 30

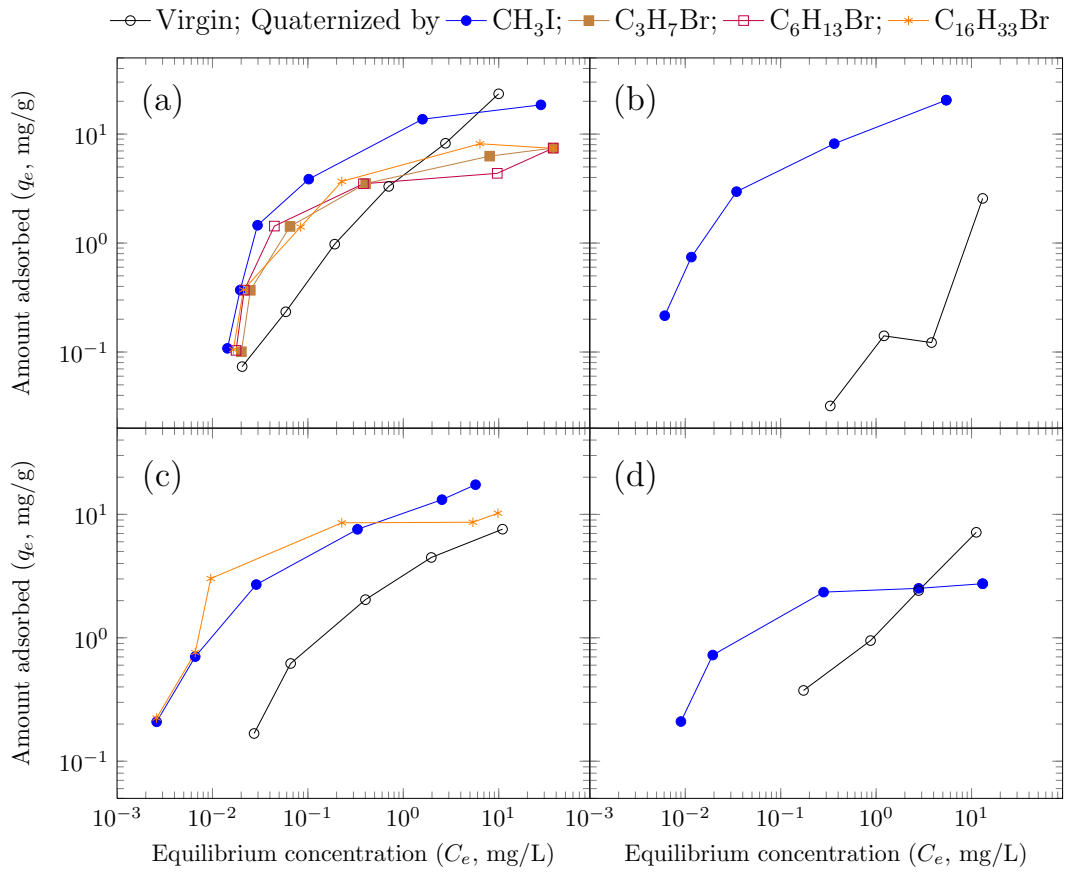

Figure 5.22: Perchlorate adsorption isotherm by virgin and quaternized carbons for (a) AC1240C, (b) GC, (c) UC1240, and (d) RGC. (Data from Tim Byrne and Pin hou)

ppb at 1,500 BV. While the quaternized UC1240 was able to remove perchlorate to below detection for 5,500 BV, 6 times longer than virgin UC1240 and full breakthrough for 6,500 BV. Similar trends were observed for other type of carbons. It is interesting to note that perchlorate exhibited an immediately breakthrough for virgin GC carbon, while the BV value for quaternized samples was around 1,500.

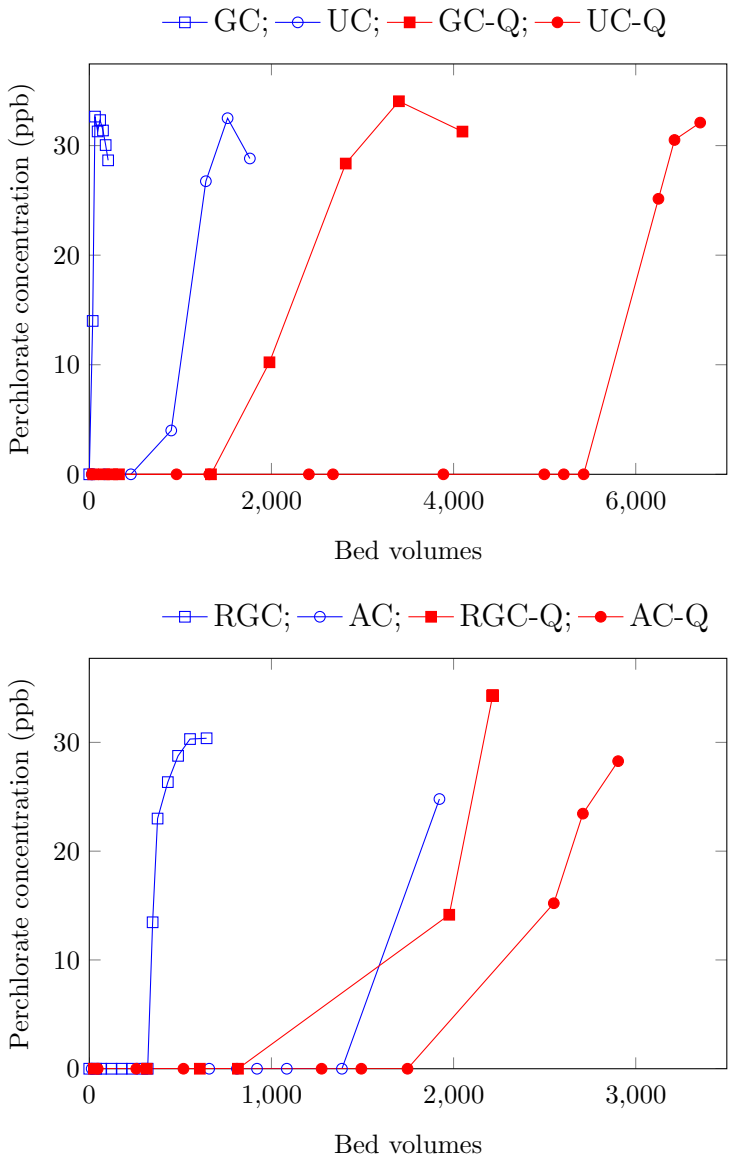

Figure 5.23: RSSCTs of perchlorate breakthrough by virgin and quaternized carbons (samples marked by designation Q, Data from Tim Byrne and Pin hou)

Chapter 6

Conclusion and Future Work

6.1 Conclusion

- The XPS studies indicated that the nitric acid oxidation generates a significantly large number of surface functional groups such as carbonyl, carboxyl, and phenol groups. The nitric acid oxidation also created negatively charged sites as it lowered the slurry pH and promoted the removal of methylene blue dye adsorption.

- Surface elemental analysis (by X-ray photoelectron spectroscopy, XPS) results showed that nitrogen was incorporated into the carbon matrix as high as 7.2% (atomic percentage) during the amination. The temperature of the ammonia treatment, the degree of pre-oxidation and the fraction of ammonia in the carrier gas influenced the population of nitrogen species. Based on the XPS study on N1s spectrum at different amination temperature, it is suspected that during the initial stages of heating, some intermediates such as amide, lactam and imide were formed. As temperature increased, these labile species were converted to more thermodynamically stable structures with heterocyclic aromatic moieties (pyridinic or pyrrolic functional groups). At higher temperature ($>$ 600 °C), the fraction of quaternary nitrogen gradually increased, but some nitrogen species might have decomposed. As little as 5% ammonia in the carrier gas was able to achieve a nitrogen content of 6.7 %.

- XPS in conjunction with chemical derivatization (by methyl iodide) was confirmed to be an effective way to qualitatively analyze the pyridinium species.

- Through quaternization, pyridine groups at edge sites were successfully transformed to pyridinium groups.

- With regard to sample porosity, Nitric acid treatment led to an appreciable loss of the total surface area and a small increase in the mesopore volume with some widening of the average pore width. Amination caused a considerable increase in surface area of the activated carbons with enhanced pore widening compared to the pre-oxidized carbons. After quaternization, the surface area and the volumes of micropores and mesopores decreased considerably for all the carbon samples.
- Pyridinium-tailored carbons achieved as much as a 6-fold improvement in bed life for adsorbing perchlorate as determined by rapid small-scale column tests (RSSCT) using spiked groundwater with perchlorate (30 ppb).

6.2 Future Work

- Use more specific techniques (like ^{15}N solid NMR) to characterize the pyridinium species.
- Test other alkylating reagents other than methyl iodide, which is not appropriate for large scale usage.
- Set up field-scale trials of pyridinium-tailored carbons.

Bibliography

American Water Works Association (1999) Water Quality & Treatment Handbook. McGraw-Hill Professional.

Arrigo, R., Havecker, M., Wrabetz, S., Blume, R., Lerch, M., McGregor, J., Parrott, E. P. J., Zeitler, J. A., Gladden, L. F., Knop-Gericke, A., Schlogl, R. & Su, D. S. (2010) Tuning the acid/base properties of nanocarbons by functionalization via amination. J. Am. Chem. Soc. 132(28):9616–9630.

Ayala, P., Arenal, R., Rummeli, M., Rubio, A. & Pichler, T. (2010) The doping of carbon nanotubes with nitrogen and their potential applications. Carbon 48(3):575–586.

Bandosz, T. J. (2006) Activated Carbon Surfaces in Environmental Remediation, Volume 7 (Interface Science and Technology). Academic Press.

Bansal, R. C. & Goyal, M. (2005) Activated Carbon Adsorption. CRC Press.

Bartle, K. D., Perry, D. L. & Wallace, S. (1987) The functionality of nitrogen in coal and derived liquids - an XPS study. Fuel Process. Technol. 15:351–361.

Biniak, S., Szymanski, G., Siedlewski, J. & Swiatkowski, A. (1997) The characterization of activated carbons with oxygen and nitrogen surface groups. Carbon 35(12):1799–1810.

Boehm, H. (1966) Chemical identification of surface groups. In: D.D. Eley, H. P. & Weisz, P. B. (eds.), Advances in Catalysis, Academic Press, vol. 16, pp. 179–274.

Brandhuber, P. & Clark, S. (2005) Perchlorate occurrence mapping. Tech. rep., American Water Works Association.

Casanovas, J., Ricart, J. M., Rubio, J., Illas, F. & JimenezMateos, J. M. (1996) Origin of the large n is binding energy in x-ray photoelectron spectra of calcined carbonaceous materials. J. Am. Chem. Soc. 118(34):8071–8076.

Charnley, G. (2008) Perchlorate: Overview of risks and regulation. Food Chem. Toxicol. 46(7):2307–2315.

Chen, W. F. & Cannon, F. S. (2005) Thermal reactivation of ammonia-tailored granular activated carbon exhausted with perchlorate. Carbon 43(13):2742–2749.

Chen, W. F., Cannon, F. S. & Rangel-Mendez, J. R. (2005a) Ammonia-tailoring of GAC to enhance perchlorate removal. I: Characterization of NH_3 thermally tailored GACs. Carbon 43(3):573–580.

Chen, W. F., Cannon, F. S. & Rangel-Mendez, J. R. (2005b) Ammonia-tailoring of GAC to enhance perchlorate removal. II: Perchlorate adsorption. Carbon 43(3):581–590.

Chingombe, P., Saha, B. & Wakeman, R. J. (2005) Surface modification and characterisation of a coal-based activated carbon. Carbon 43(15):3132–3143.

de la Puente, G., Pis, J. J., Menendez, J. A. & Grange, P. (1997) Thermal stability of oxygenated functions in activated carbons. J. Anal. Appl. Pyrolysis 43(2):125–138.

Desimoni, E., Casella, G. I., Salvi, A. M., Cataldi, T. R. I. & Morone, A. (1992) Xps investigation of ultra-high-vacuum storage effects on carbon-fiber surfaces. Carbon 30(4):527–531.

El-Sayed, Y. & Bandosz, T. J. (2005) Role of surface oxygen groups in incorporation of nitrogen to activated carbons via ethylmethylamine adsorption. Langmuir 21(4):1282–1289.

Estrade-Szwarckopf, H. (2004) Xps photoemission in carbonaceous materials: A "defect" peak beside the graphitic asymmetric peak. Carbon 42(8-9):1713–1721.

Figueiredo, J. L., Pereira, M. F. R., Freitas, M. M. A. & Orfao, J. J. M. (1999) Modification of the surface chemistry of activated carbons. Carbon 37(9):1379–1389.

Grzybek, T. & Kreiner, K. (1997) Surface changes in coals after oxidation .1. x-ray photoelectron spectroscopy studies. Langmuir 13(5):909–912.

Gu, B. & Coates, J. D. (2006) Perchlorate: Environmental Occurrence, Interactions and Treatment. Springer.

Gu, B., Ku, Y.-K. & Brown, G. M. (2002) Treatment of perchlorate-contaminated groundwater using highly selective, regenerable ion-exchange technology: A pilot-scale demonstration. Remediation 12(2):51–68.

Gu, B. H., Brown, G. M., Maya, L., Lance, M. J. & Moyer, B. A. A. (2001) Regeneration of perchlorate (ClO_4^-)-loaded anion exchange resins by a novel tetrachloroferrate ($FeCl_4^-$) displacement technique. Environ. Sci. Technol. 35(16):3363–3368.

Gu, B. H., Brown, G. M. & Chiang, C. C. (2007) Treatment of perchlorate-contaminated groundwater using highly selective, regenerable ion-exchange technologies. Environ. Sci. Technol. 41(17):6277–6282.

Hagström, E. (2006) Perchlorate: a scientific, legal, and economic assessment. Lawyers and Judges Publishing.

Jansen, R. J. J. & van Bekkum, H. (1994) Amination and ammoxidation of activated carbons. Carbon 32(8):1507–1516.

Kelemen, S. R., Gorbaty, M. L. & Kwiatek, P. J. (1994) Quantification of nitrogen forms in argonne premium coals. Energy & Fuels 8(4):896–906.

Kozlowski, C. & Sherwood, P. M. A. (1985) X-ray photoelectron-spectroscopic studies of carbon-fibre surfaces .5. the effect of ph on surface oxidation. Journal of the Chemical Society-faraday Transactions I 81:2745–2756.

Krupa, N. E. & Cannon, F. S. (1996) Gac: Pore structure versus dye adsorption. J Am Water Works Assoc 88(6):94–108.

Kucharzyk, K. H., Crawford, R. L., Cosens, B. & Hess, T. F. (2009) Development of drinking water standards for perchlorate in the united states. J. Environ. Manage. 91(2):303–310.

Kundu, S., Xia, W., Busser, W., Becker, M., Schmidt, D. A., Havenith, M. & Muhler, M. (2010) The formation of nitrogen-containing functional groups on carbon nanotube surfaces: a quantitative xps and tpd study. Phys. Chem. Chem. Phys. 12(17):4351–4359.

Lahaye, J., Nanse, G., Fioux, P., Bagreev, A., Broshnik, A. & Strelko, V. (1999) Chemical transformation during the carbonisation in air and the pyrolysis under argon of a vinylpyridine-divinylbenzene copolymer by x-ray photoelectron spectroscopy. Appl. Surf. Sci. 147(1-4):153–174.

Li, H. F., Xi, H. A., Zhu, S. M., Wen, Z. Y. & Wang, R. D. (2006) Preparation, structural characterization, and electrochemical properties of chemically modified mesoporous carbon. Microporous Mesoporous Mater. 96(1-3):357–362.

Li, X. L., Wang, H. L., Robinson, J. T., Sanchez, H., Diankov, G. & Dai, H. J. (2009) Simultaneous nitrogen doping and reduction of graphene oxide. J. Am. Chem. Soc. 131(43):15939–15944.

Liu, F., Gentles, A. & Theodorakis, C. W. (2008) Arsenate and perchlorate toxicity, growth effects, and thyroid histopathology in hypothyroid zebrafish danio rerio. Chemosphere 71(7):1369–1376.

Logan, B. E. (2001) Assessing the outlook for perchlorate remediation. Environ. Sci. Technol. 35(23):482A–487A.

Mahmudov, R. & Huang, C. P. (2010) Perchlorate removal by activated carbon adsorption. Sep. Purif. Technol. 70(3):329–337.

Maldonado, S., Morin, S. & Stevenson, K. J. (2006) Structure, composition, and chemical reactivity of carbon nanotubes by selective nitrogen doping. Carbon 44(8):1429–1437.

Mangun, C. L., Benak, K. R., Daley, M. A. & Economy, J. (1999) Oxidation of activated carbon fibers: Effect on pore size, surface chemistry, and adsorption properties. Chem. Mater. 11(12):3476–3483.

Mangun, C. L., Benak, K. R., Economy, J. & Foster, K. L. (2001) Surface chemistry, pore sizes and adsorption properties of activated carbon fibers and precursors treated with ammonia. Carbon 39(12):1809–1820.

Menendez, J. A., Phillips, J., Xia, B. & Radovic, L. R. (1996) On the modification and characterization of chemical surface properties of activated carbon: In the search of carbons with stable basic properties. Langmuir 12(18):4404–4410.

Moore, B. C., Cannon, F. S., Metz, D. H. & Demarco, J. (2003) Gac pore structure in cincinnati - during full-scale treatment/reactivation. J Am Water Works Assoc 95(2):103–112.

Moreno-Castilla, C., Ferro-Garcia, M. A., JOLY, J. P., Bautista-Toledo, I., Carrasco-Marin, F. & Rivera-Utrilla, J. (1995) Activated carbon surface modifications by nitric-acid, hydrogen-peroxide, and ammonium peroxydisulfate treatments. Langmuir 11(11):4386–4392.

Moreno-Castilla, C., Lopez-Ramon, M. V. & Carrasco-Marin, F. (2000) Changes in surface chemistry of activated carbons by wet oxidation. Carbon 38(14):1995–2001.

Motzer, W. E. (2001) Perchlorate: Problems, detection, and solutions. Environmental Forensics 2(4):301–311.

Na, C. Z., Cannon, F. S. & Hagerup, B. (2002) Perchlorate removal via iron-preloaded gac and borohydride regeneration. J Am Water Works Assoc 94(11):90–102.

Parette, R. & Cannon, F. S. (2005) The removal of perchlorate from groundwater by activated carbon tailored with cationic surfactants. Water Res. 39(16):4020–4028.

Parette, R., Cannon, F. S. & Weeks, K. (2005) Removing low ppb level perchlorate, rdx, and hmx from groundwater with cetyltrimethylammonium chloride (ctac) pre-loaded activated carbon. Water Res. 39(19):4683–4692.

Paulus, B. F., Bazar, M. A., Salice, C. J., Mattie, D. R. & Major, M. A. (2007) Perchlorate inhibition of iodide uptake in normal and iodine-deficient rats. J. Toxicol. Environ. Health, Part A 70(13):1142–1149.

Perez-Cadenas, M., Moreno-Castilla, C., Carrasco-Marin, F. & Perez-Cadenas, A. F. (2009) Surface chemistry, porous texture, and morphology of n-doped carbon xerogels. Langmuir 25(1):466–470.

Perrier, D. M. & Benerito, R. R. (1975) Mono- and diquaternary ammonium cellulose cottons prepared in nonaqueous media. J. Appl. Polym. Sci. 19(12):3211–3220.

Pietrzak, R., Jurewicz, K., Nowicki, P., Babel, K. & Wachowska, H. (2007) Microporous activated carbons from ammoxidised anthracite and their capacitance behaviours. Fuel 86(7-8):1086–1092.

Pittman, C. U., He, G. R., Wu, B. & Gardner, S. D. (1997) Chemical modification of carbon fiber surfaces by nitric acid oxidation followed by reaction with tetraethylenepentamine. Carbon 35(3):317–331.

Radovic, L. R. (2008) Chemistry and Physics of Carbon, vol. 30. CRC Press.

Rangel-Mendez, J. R. & Cannon, F. S. (2005) Improved activated carbon by thermal treatment in methane and steam: Physicochemical influences on mib sorption capacity. Carbon 43(3):467–479.

Russell, C. G., Roberson, J. A., Chowdhury, Z. & McGuire, M. J. (2009) National cost implications of a perchlorate regulation. J Am Water Works Assoc 101(3):54–67.

Seredych, M., Hulicova-Jurcakova, D., Lu, G. Q. & Bandosz, T. J. (2008) Surface functional groups of carbons and the effects of their chemical character, density and accessibility to ions on electrochemical performance. Carbon 46(11):1475–1488.

Shi, Z., Neoh, K. G. & Kang, E. T. (2007) Antibacterial and adsorption characteristics of activated carbon functionalized with quaternary ammonium moieties. Ind. Eng. Chem. Res. 46(2):439–445.

Srinivasan, A. & Viraraghavan, T. (2009) Perchlorate: Health effects and technologies for its removal from water resources. Int J Environ Res Public Health 6(4):1418–1442.

Srinivasan, R. & Sorial, G. A. (2009) Treatment of perchlorate in drinking water: A critical review. Sep. Purif. Technol. 69(1):7–21.

Stanczyk, K., Dziembaj, R., Piwowarska, Z. & Witkowski, S. (1995) Transformation of nitrogen structures in carbonization of model compounds determined by xps. Carbon 33(10):1383–1392.

Stohr, B., Boehm, H. P. & Schlogl, R. (1991) Enhancement of the catalytic activity of activated carbons in oxidation reactions by thermal-treatment with ammonia or hydrogen-cyanide and observation of a superoxide species as a possible intermediate. Carbon 29(6):707–720.

Tripp, A. R. & Clifford, D. A. (2006) Ion exchange for the remediation of perchlorate-contaminated drinking water. J Am Water Works Assoc 98(4):105–114.

Urbansky, E. T. (1998) Perchlorate chemistry: Implications for analysis and remediation. Bioremediation Journal 2(2):81–95.

Urbansky, E. T. (2002) Perchlorate as an environmental contaminant. Environ. Sci. Pollut. Res. 9(3):187–192.

U.S. General Accountability Office (2007) Environmental contamination department of defense activities related to trichloroethylene, perchlorate, and other emerging contaminants. Tech. rep.

Vickerman, J. C. & Gilmore, I. (2009) Surface Analysis: The Principal Techniques. Wiley, 2nd edn.

Wang, X. Q., Lee, J. S., Zhu, Q., Liu, J., Wang, Y. & Dai, S. (2010) Ammonia-treated ordered mesoporous carbons as catalytic materials for oxygen reduction reaction. Chem. Mater. 22(7):2178–2180.

Wepasnick, K. A., Smith, B. A., Schrote, K. E., Wilson, H. K., Diegelmann, S. R. & Fairbrother, D. H. (2011) Surface and structural characterization of multi-walled carbon nanotubes following different oxidative treatments. Carbon 49(1):24–36.

Xiao, Y. Y., Basu, A., Kashyap, V. & Roberts, D. J. (2010) Experimental and numerical analysis of biological regeneration of perchlorate laden ion-exchange resins in batch reactors. Environ. Eng. Sci. 27(1):75–84.

Xie, F., Phillips, J., Silva, I. F., Palma, M. C. & Menendez, J. A. (2000) Microcalorimetric study of acid sites on acid-pretreated activated carbon. Carbon 38(5):691–700.

Xiong, Z., Zhao, D. & Harper, W. F. (2007) Sorption and desorption of perchlorate with various classes of ion exchangers: A comparative study. Ind. Eng. Chem. Res. 46(26):9213–9222.

Yoon, I. H., Meng, X. G., Wang, C., Kim, K. W., Bang, S., Choe, E. & Lippincott, L. (2009) Perchlorate adsorption and desorption on activated carbon and anion exchange resin. J. Hazard. Mater. 164(1):87–94.

Zewdie, T., Smith, C. M., Hutcheson, M. & West, C. R. (2010) Basis of the massachusetts reference dose and drinking water standard for perchlorate. Environ. Health Perspect. 118(1):42–48.

Zielke, U., Huttinger, K. J. & Hoffman, W. P. (1996) Surface-oxidized carbon fibers .1. surface structure and chemistry. Carbon 34(8):983–998.